minerals

MDPI

Article

Prospecting Prediction Model and Target Delineation of "Dongchuan-Type" Copper Deposits in the SW Yangtze Block: A Case Study of the Shizishan Deposit, Yunnan Province

Xiaofei Zhang [1,2,*], Junlu Wang [1,2], Hui Chen [1,2,*], Zhenshan Pang [1,2], Bing Yu [1,2], Guochao Chen [3] and Xiatao Wu [4]

[1] Development and Research Centre, China Geological Survey, Beijing 100037, China; wangjunlu2007@126.com (J.W.)
[2] Mineral Exploration Technical Guidance Center, Ministry of Natural Resources, Beijing 100037, China
[3] School of Civil Engineeringy, Nanyang Institute of Technology, Nanyang 473000, China
[4] Yunnan Copper Mineral Resources Exploration and Development Co., Ltd., Kunming 650000, China; txwxt@chinalco.com.cn
* Correspondence: zhangxiaofei521125@163.com (X.Z.); cgschenhui@163.com (H.C.)

Abstract

Amidst the intensification of strategic mineral exploration, the discovery of concealed and deep-seated deposits within covered areas and the peripheries of existing mines has become a critical challenge and a central focus of contemporary research. "Dongchuan-type" (DCT) copper deposits represent a key mineralization style within the SW Yangtze Block. However, significant exploration breakthroughs have stagnated over the past three decades. Consequently, advanced exploration prediction research is urgently required to guide deep-resource evaluation. Using the Shizishan copper deposit in the Yimen area as a representative case, this study applies the theory of "metallogenic geological body prediction" to construct a tripartite model encompassing "metallogenic geological bodies, metallogenic structures and structural planes, and metallogenic characteristic markers". The Shizishan deposit is classified as a sedimentary-reformed type, characterized by multi-episodic mineralization involving initial sedimentary processes, non-magmatic hydrothermal activity, and subsequent structural-magmatic hydrothermal overprinting. Key metallogenic geological bodies include ore-bearing stratigraphic associations, basin-margin faults, NE-trending fold–fault systems, and deep-seated concealed intrusions. Metallogenic structural planes comprise primary ore-controlling surfaces, secondary fold-related structures, and potential deep-seated magmatic intrusive interfaces. Alteration patterns display a distinct vertical zonation: shallower levels show medium-to-low temperature hydrothermal processes (silicification, carbonatization, sericitization, and chloritization), whereas deeper portions reveal high-temperature magmatic–hydrothermal indicators, specifically skarnization and intense silicification. This study proposes that the integration of "stratigraphy + structures + concealed intrusions" should serve as the primary criterion for target screening in deep exploration. By integrating geophysical and geochemical datasets into this model, three promising exploration targets were delineated within the Yimen area. These findings provide a refined theoretical framework for large-scale prospecting of DCT.

Keywords: "Dongchuan-type" copper deposits; Shizishan deposit; metallogenic geological body theory; exploration prediction; target delineation

Check for updates

Academic Editor: Majid Ghaderi

Received: 26 April 2026
Revised: 5 August 2026
Accepted: 6 August 2026
Published: 11 August 2026

Copyright: © 2026 by the authors. Licensee MDPI, Basel, Switzerland. This article is an open access article distributed under the terms and conditions of the Creative Commons Attribution (CC BY) license.

1. Introduction

Mineral exploration is a multifaceted and high-risk endeavor that occupies a foundational position in the industrial chain of mineral resource development and utilization [1]. With the intensification of global exploration, most outcropping and shallow-seated deposits have already been largely depleted. Therefore, the discovery of concealed and deep-seated ore bodies has emerged as a scientific frontier and a priority for the global exploration community. Large-scale mineral exploration prediction not only facilitates direct prospecting efforts but also serves as a critical pathway for advancing scientific exploration methodologies [2]. To address these increasing challenges of finding deep or concealed mineral deposits, scholars worldwide have developed various metallogenic prognosis theories. These include the prediction–prospecting assemblage theory, ore-deposit model prediction, metallogenic system theory, metallogenic series theory, and metallogenic geological body prospecting prediction theory (MGBT, also referred to as the "exploration-area" theory and methodology) [1–6]. Furthermore, statistical approaches and ore-body localization based on geological anomalies have been widely applied [5]. Among these, the MGBT, pioneered by the research team of Prof. Ye Tianzhu, integrates geochemical, mineralogical, and economic geology studies with practical exploration strategies. The core of this methodology is the "Three-in-One" (or "Trinity") prospecting–prediction model, which synthesizes three critical components: the metallogenic geological body, metallogenic structures and structural planes, and metallogenic characteristic markers. This framework provides both the theoretical guidance and the methodological protocols necessary for exploration within specific districts [1,2,6]. Guided by the MGBT, significant breakthroughs were achieved in China between 2012 and 2021, in particular, in the deep and peripheral zones of 168 existing mining operations. This led to notable success across 83 ore-concentrated districts and 141 integrated exploration areas, resulting in the "five-new" advancements: new districts, new horizons, new deposit types, new commodities, and new depths [1,6,7].

The Kangdian Rift zone, situated on the southwestern margin of the Yangtze Block, is a vital copper–iron polymetallic metallogenic belt in China [8]. This belt hosts several prominent copper ore clusters, including the Lala cluster in Sichuan Province and the Dongchuan, Wuding, Yimen, and Dahongshan districts in Yunnan Province (Figure 1b). Characterized by favorable geological conditions for large-scale mineralization, the region has become the focus of intensive exploration and research since the 1960s. These research efforts have led to a sequence of exploration successes, with identified copper resources totaling approximately 10 million tons. However, with the progress of exploration, shallow-seated mineral resources have been largely depleted. Consequently, covered areas and the deep-seated peripheral zones of existing mines have become the primary targets for future breakthroughs. In recent years, significant progress has been recorded in the deep and peripheral areas of the Lala copper deposit in Huili, Sichuan, where over 1 Mt of additional copper resources have been identified [7]. In stark contrast, no major exploration advances have been achieved in the Dongchuan–Wuding–Yimen copper districts over the past three decades. This prolonged stagnation underscores the urgent need for innovative prospecting prediction research to guide the next-generation deep-resource exploration and evaluation in these areas.

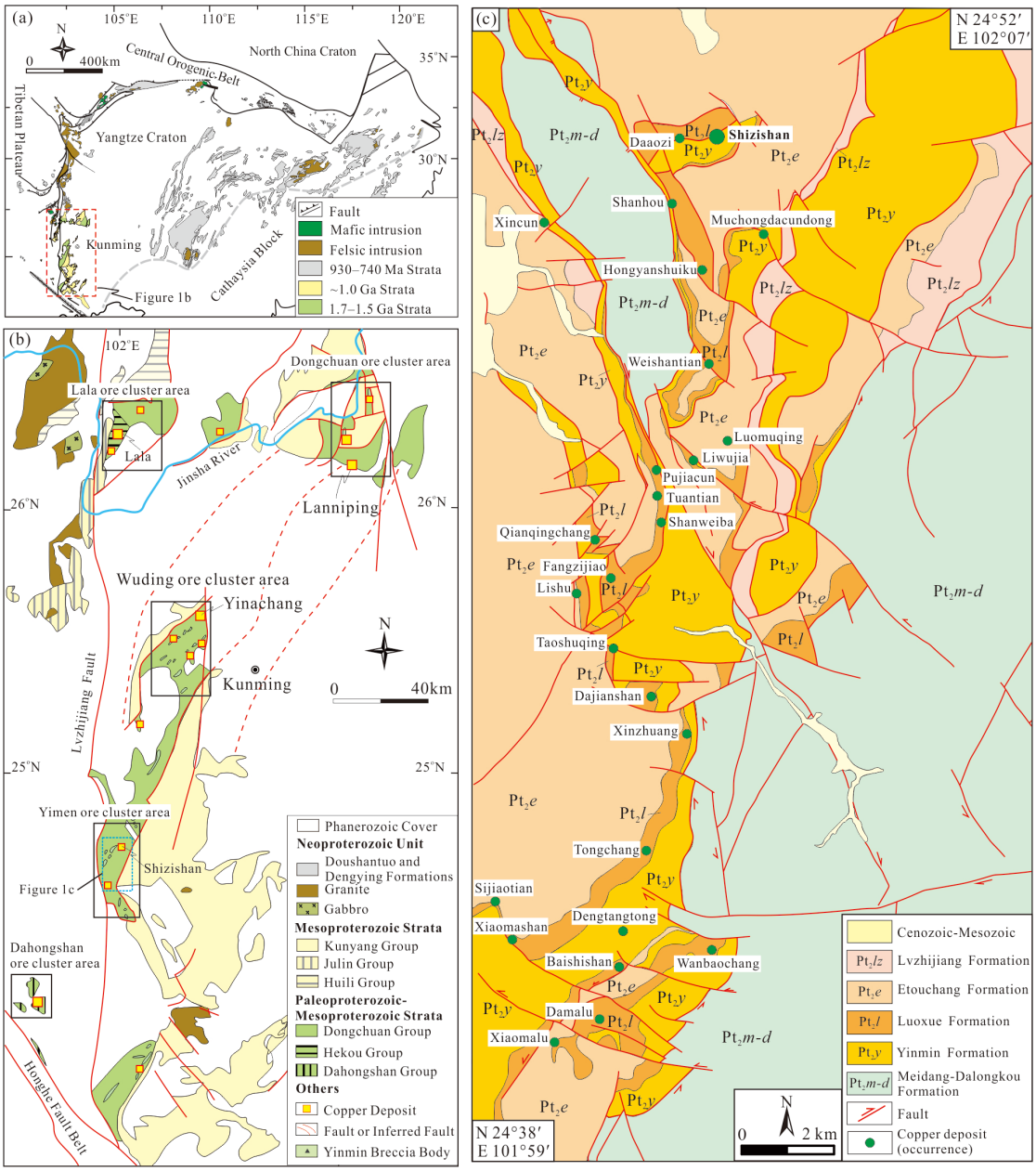


Figure 1. Tectonic setting and regional geology of the Kangdian region and the study area: (**a**) map showing the tectonic location of the Kangdian region; (**b**) simplified geological map of the Kangdian region (adapted from references [7,9]); (**c**) geological map of the SZS area in Yimen, Yunnan Province (adapted from reference [10]).

The Dongchuan–Wuding–Yimen district is characterized by "Dongchuan-type" (DCT) copper deposits, which represent Proterozoic rift-related sediment-hosted stratiform copper deposits [11–13]. These exhibit metallogenic settings and mineralization characteristics comparable to those of world-class sediment-hosted copper systems, including the Central African Copperbelt (Zambia–Congo copper–cobalt belt) and the White Pine deposit in North America [14–26]. The DCT copper deposits are primarily hosted in: (i) the basal dolomite of the Luoxue Formation (Fm.; Dongchuan Group); (ii) the transitional zone between the Luoxue and Etouchang Formations (locally referred to as the Heishan Fm.); and (iii) the transitional zone between the Luoxue and Yinmin Formations [11,12]. Representative large- to medium-sized deposits include Tangdan, Dongchuan, Luoxue, Shifengshan, and Shizishan (SZS) copper deposits [11,13]. Extensive research has addressed the met-

allogenic settings, regularities, fluid/material sources, and genesis of the DCT [14–23]. Nonetheless, significant controversies persist. Regarding deposit genesis, classification has historically varied based on perceived fluid sources and the relationship between mineralization and sedimentation. Prior to the 1960s, the prevailing perspective was that the rocks had a metasomatic origin, driven by mafic magmatic–hydrothermal fluids along bedding planes. In the 1970s, a sedimentary–metamorphic model was proposed, suggesting the formation of orebodies through the remobilization and reprecipitation of metals during regional metamorphism. By the 1980s, more diverse theories emerged, including marine exhalative-sedimentary, sedimentary-reworked, and sedimentary-activated hydrothermal remobilization origin [11,19,21,22]. Since 2000, a polygenetic-compound origin has been increasingly advocated, emphasizing the overprinting of original mineralization by subsequent tectonism and magmatic–hydrothermal activity [14]. Post-2010, many researchers have increasingly adopted a basin-brine metasomatic model [18,20]. Some argue that mineralization occurred primarily during the sedimentary-diagenetic stage, potentially overprinted by later events [18,24–29], while others contend that ore formation was largely driven by post-diagenetic basin closure and orogenic processes [30–32]. These evolving genetic models have directly influenced exploration strategies. Between the 1960s and 1980s, several empirical models were proposed for specific mining sites, notably the Dongchuan, Fengshan, Shishan, Xikuangshan, and Taoyuan types. This proliferation of "one-deposit–one-model" nomenclature often hindered regional correlation and a unified understanding of the belt. In the 1990s, the "Four-Level, One-Ladder" model was introduced within the framework of metallogenic series. This model proposed that the diverse copper deposit types constitute a comprehensive rift-related metallogenic system, and it emphasized the importance of pursuing multi-horizon exploration [11]. Since 2010, redox interfaces have been recognized as the primary factor controlling orebody localization, with an additional emphasis on the role of late-stage tectonic reworking in ore enrichment [14,17,18,20,27]. Despite these advancements, practical exploration remains heavily concentrated on the Luoxue Fm. A comprehensive understanding of orebodies in other stratigraphic levels and their governing ore-controlling factors, remains largely underdeveloped. Furthermore, the scarcity of integrated prospecting prediction models for these complex systems continues to impede breakthroughs in regional mineral exploration.

The SZS copper deposit in the Yimen area exemplifies classic DCT-type mineralization. It is characterized by both stratigraphic and structural controls, and has experienced substantial late-stage reworking and enrichment [14,33]. Guided by the MGBT [2], this study focuses on the SZS deposit as its primary research subject. Drawing on both a synthesis of existing literature and new field observations, the metallogenic geological bodies, structural systems and interfaces, and characteristic markers of the SZS deposit were systematically evaluated. This analysis was used to construct a "Three-in-One" (Trinity) prospecting prediction model and to establish comprehensive prospecting criteria. Finally, by integrating geophysical and geochemical data with the proposed model, a targeted prospecting prediction was conducted in this study, providing a modernized and effective framework for exploring deep-seated DCT in the region.

2. Metallogenic Geological Setting

2.1. Regional Geological Setting

The Kangdian Rift zone lies along the SW margin of the Yangtze Block. It is bounded by the Sanjiang Orogenic Belt to the west, the Ailaoshan Fault Zone to the south, and the Longmenshan Fault Zone to the north [34]. The region has experienced a complex, multi-stage evolutionary history, including basement formation, cover sequence development and stabilization, continental rifting, and subsequent intracontinental reworking [14,35–47]. Suc-

cessive episodes of tectonic–magmatic activity, coupled with metamorphic–deformational processes have established highly favorable conditions for mineralization. Extensive early Mesoproterozoic sequences, deposited within an intracontinental rift setting, most notably the Dahongshan, Dongchuan, and Hekou groups, host the primary Cu–Fe–Co ore horizons in the region [8,48,49].

The Yimen copper ore district is located in the central Kangdian Rift zone, situated within a fault-bounded basin between the regional Lvzhijiang and Yimen faults. This Yimen fault-depression basin forms part of the Wuding–Yimen–Yuanjiang rift trough within the broader Kunyang Rift system (Figure 1b). The Proterozoic Dongchuan Group represents the predominant stratigraphic unit exposed in the area and is sequentially subdivided from base to top into the Yinmin, Luoxue, Etouchang, and Lvzhijiang formations (Figure 1c). These units display conformable contacts and were deposited between approximately 1.74 and 1.50 Ga, later experiencing greenschist-facies metamorphism [17]. The Mesoproterozoic Yinmin Fm. consists of purplish–gray to flesh–red sandstone, siltstone, and slate interbedded with argillaceous dolomitic limestone. The presence of evaporites identifies this as a continental red-bed unit [22,50]. Overlying this, the Luoxue Fm. is composed of light gray, grayish–white, and light flesh-red dolomites. This formation is characterized by abundant *Conophyton gaubitza* Krylov stromatolites, representing a transgressive sequence spanning upper-intertidal to subtidal facies. The Etouchang Fm. (regionally referred to as the Heishan Fm.) consists of grayish–black to black carbonaceous slate interbedded with carbonaceous–argillaceous dolomite. By contrast, the Lvzhijiang Fm. comprises gray sericite slate interbedded with sandy slate, quartz sandstone, limestone, and dolomitic lenses. The Yinmin, Luoxue, and Etouchang formations together constitute a complete transgressive succession, transitioning from basal siliciclastics to dolomitic carbonates and culminating in black carbonaceous shales. This sequence serves as the primary ore-hosting stratigraphic interval for copper mineralization in the Yimen area. The "Xikuangshan-type" deposits, hosted in the Yinmin Fm.; the "Dongchuan-type" deposits, hosted in the Luoxue Fm.; and the "Taoyuan-type" deposits, hosted in the Etouchang Fm. are developed within these three units, respectively [10,30]. This structural framework of the region is dominated by NS- and NE-trending fold-and-fault systems. Magmatic activity is represented by an early Mesoproterozoic to late Paleoproterozoic suite (1.8–1.95 Ga) consisting of diabase, gabbro, and quartz keratophyre, as well as Neoproterozoic granite (1.1–0.7 Ga) [17,51–55].

2.2. Geological Characteristics of the Mining Area

The SZS copper deposit lies along the western margin of the Yimen rift basin. The stratigraphic sequence exposed within the mining area is dominated by the Mesoproterozoic Yinmin, Luoxue, and Etouchang formations (Figure 2). Fold structures are predominantly NE- and nearly NS-trending, manifesting as a series of anticline–syncline pairs. The SZS anticlinorium, the dominant structural feature in the area, is composed of a series of subordinate, upright, and steeply plunging folds (with plunge angles between 80° and 90°) with near-vertical axial planes. The core of the anticlinorium exposes the purple clastic rocks of the Yinmin Fm., while its limbs consist of dolomite from the Luoxue Fm. and slate from the Etouchang Fm. The strata are symmetrically distributed, dipping northeast at angles of 70–80°. The orebodies of the SZS deposit are primarily hosted within the hinge zone of the anticlinorium core and in subordinate folds along its northwestern limb. Spatially, mineralization is jointly controlled by stratigraphy and structure, exhibiting both stratiform and vein-like morphologies across multiple stratigraphic levels. Host rocks include the Luoxue Fm. dolomites, Etouchang Fm. slate and dolomites, and Yinmin Fm. sandstones and slate. Notably, mineralization is also found within ferruginous dolomitic tuff interbedded with tuffaceous sandstone and dolomitic siltstone in the middle-to-upper portions of

the Yinmin Fm. (Figure 2c). Magmatic rocks in the mining area have limited exposure, consisting of minor diabase and gabbro dikes (1.5–6 m wide) intruded along fault zones. Localized chalcopyrite mineralization is observed at the margins of these dikes, where magmatic activity has either overprinted or partially redistributed pre-existing orebodies.

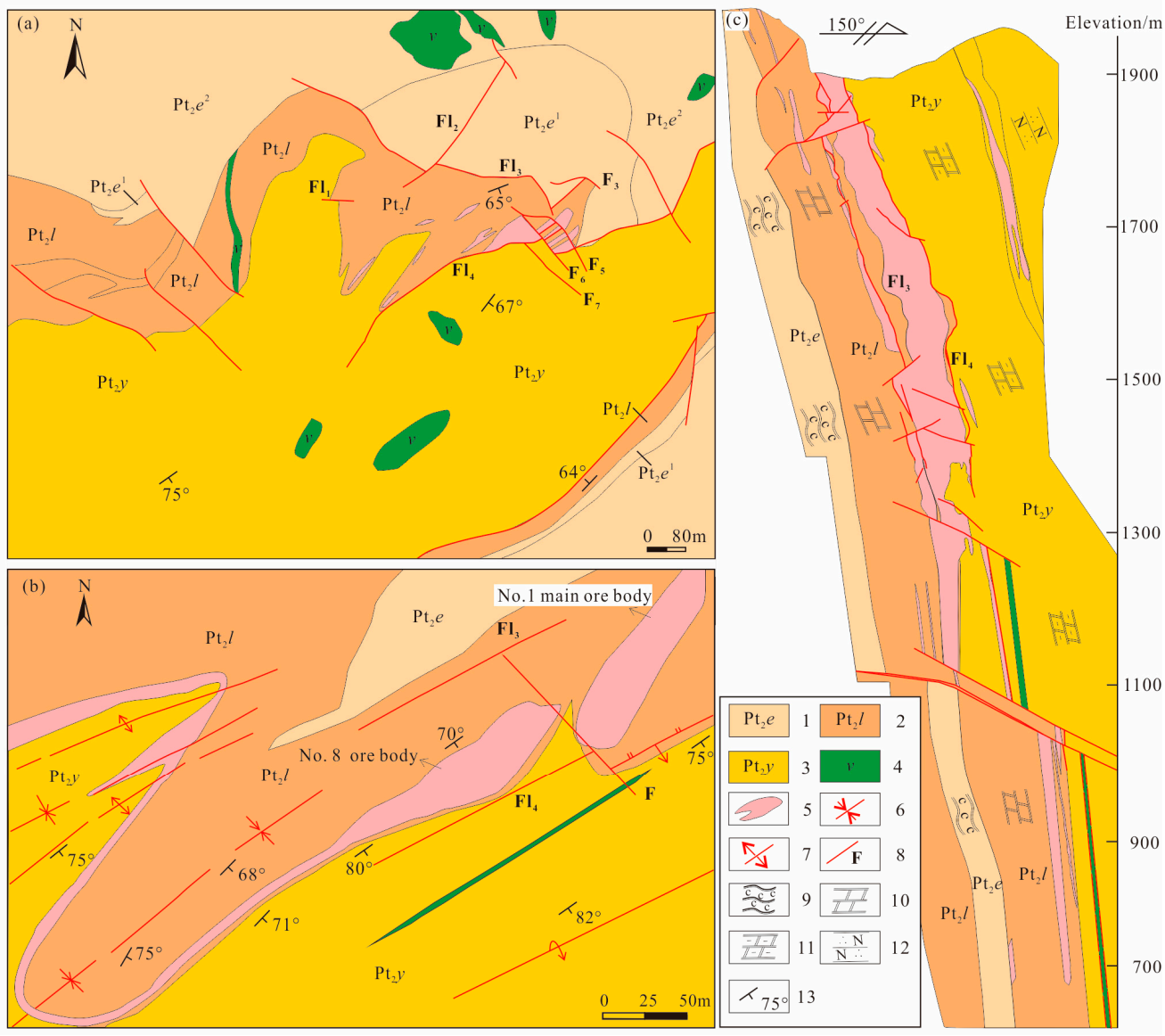


Figure 2. Geology of the SZS copper deposit: (**a**) geological map of the SZS mining area; (**b**) geological map of the middle Section 15 in the SZS copper deposit; (**c**) cross-sectional view along exploration line No. 5 (adapted from reference [33]). Legend: 1—Etouchang Fm.; 2—Luoxue Fm.; 3—Yinmin Fm.; 4—Gabbro-diabase; 5—Ore body; 6—Synclinal axis; 7—Anticlinal axis; 8—Fault and its number; 9—Carbonaceous slate; 10—Dolomite; 11—Argillaceous dolomite; 12—Feldspathic quartz sandstone; 13—Attitude.

2.3. Geophysical Characteristics

Regional gravity data indicate that the Kunyang Rift is characterized by an NS-trending gravity low, with values ranging from -175×10^{-5} to -245×10^{-5} m s^{-2}. Overall, the region exhibits localized gravity highs superimposed upon this regional negative anomaly background [56,57]. The negative background is interpreted as a reflection of a low-density crustal architecture, likely resulting from crust–mantle mixing processes occurring above the mantle. By contrast, the Yimen copper district is characterized by localized positive gravity anomalies, likely reflecting tectonic uplift of denser basement

strata. Analysis of the residual Bouguer gravity anomaly field (Figure 3a) indicates that the principal ore-bearing strata (e.g., the Luoxue Fm.) are preferentially distributed along the margins of gravity gradient zones, proximal to gravity highs.

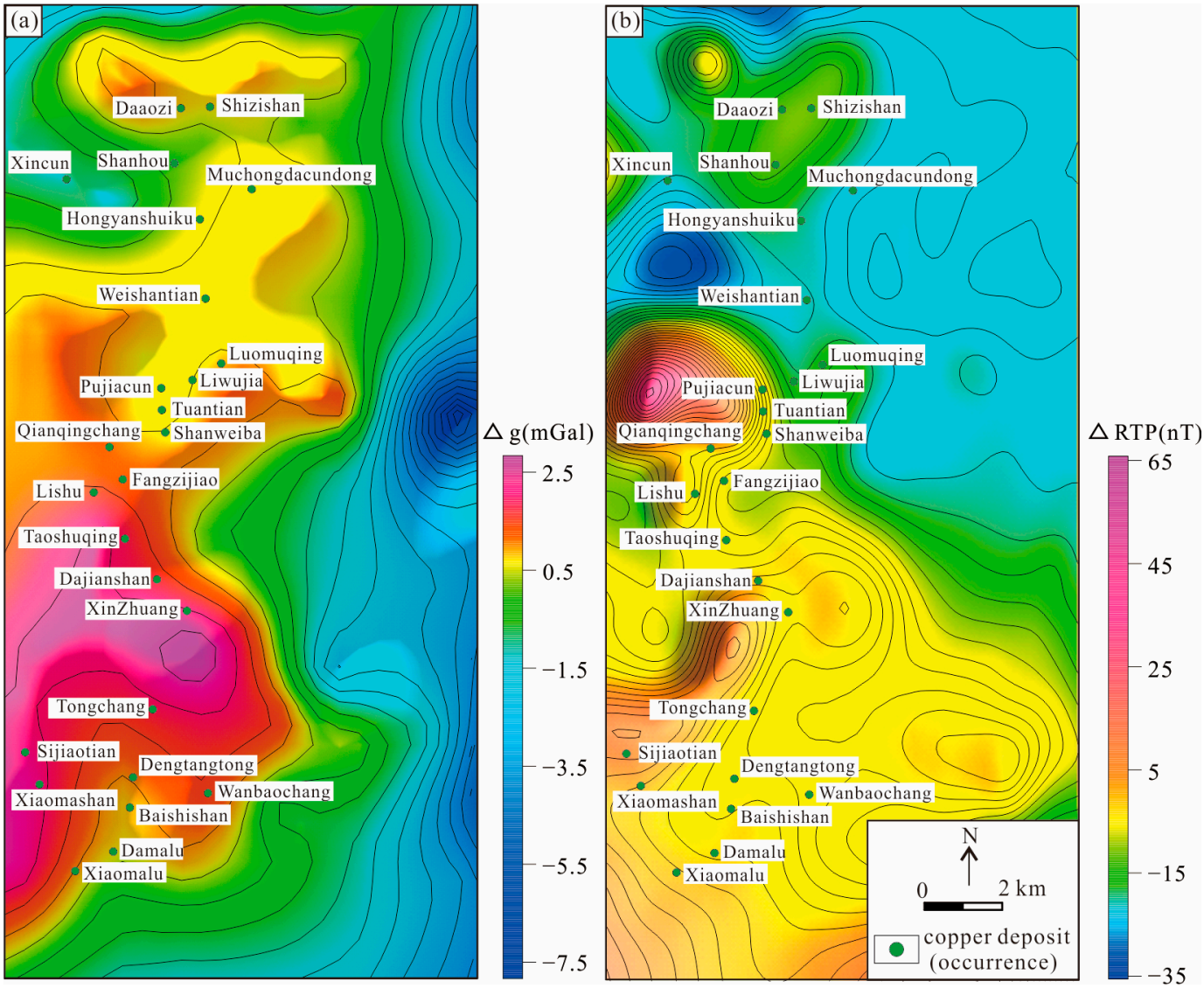


Figure 3. Geophysical anomalies in the SZS area in Yimen, Yunnan: (**a**) residual Bouguer gravity anomaly map and (**b**) residual aeromagnetic anomaly reduction to the pole map.

The 1:50,000-scale reduced-to-pole (RTP) aeromagnetic data (Figure 3b) reveals that the Yimen copper district is characterized by a moderate-to-weak magnetic field, with intensities ranging from −60 to 65 nT. Magnetic anomalies display poor lateral continuity, with sparsely distributed positive and negative anomaly centers. These characteristics are largely associated with the presence of mafic rocks, brecciated zones, structural discontinuities, and localized mineralization within the Proterozoic sequences. The majority of known mineral occurrences are spatially associated with moderate-to-high magnetic anomalies. In the SZS mining area; however, magnetic anomalies are relatively weak; this attenuated signal may be an indicator of intense hydrothermal alteration (e.g., demagnetization) or may reflect the presence of deeply buried or volumetrically minor intrusive bodies. Conversely, the more pronounced magnetic anomalies identified at the Dajianshan and Lisu copper deposits suggest a more direct association with significant magmatic–hydrothermal activity.

2.4. Geochemical Characteristics

The 1:50,000-scale geochemical survey of the SZS district reveals that the dominant elemental association is characterized by Cu, Au, Zn, and Ag, with subordinate anomalies of As, Sb, Hg, Mn, and Ni (Figure 4) [58]. The Cu anomaly displays an EW-trending, podiform distribution, extending 4 km in length and 1–2 km in width, covering an area of approximately 3.5 km^2.

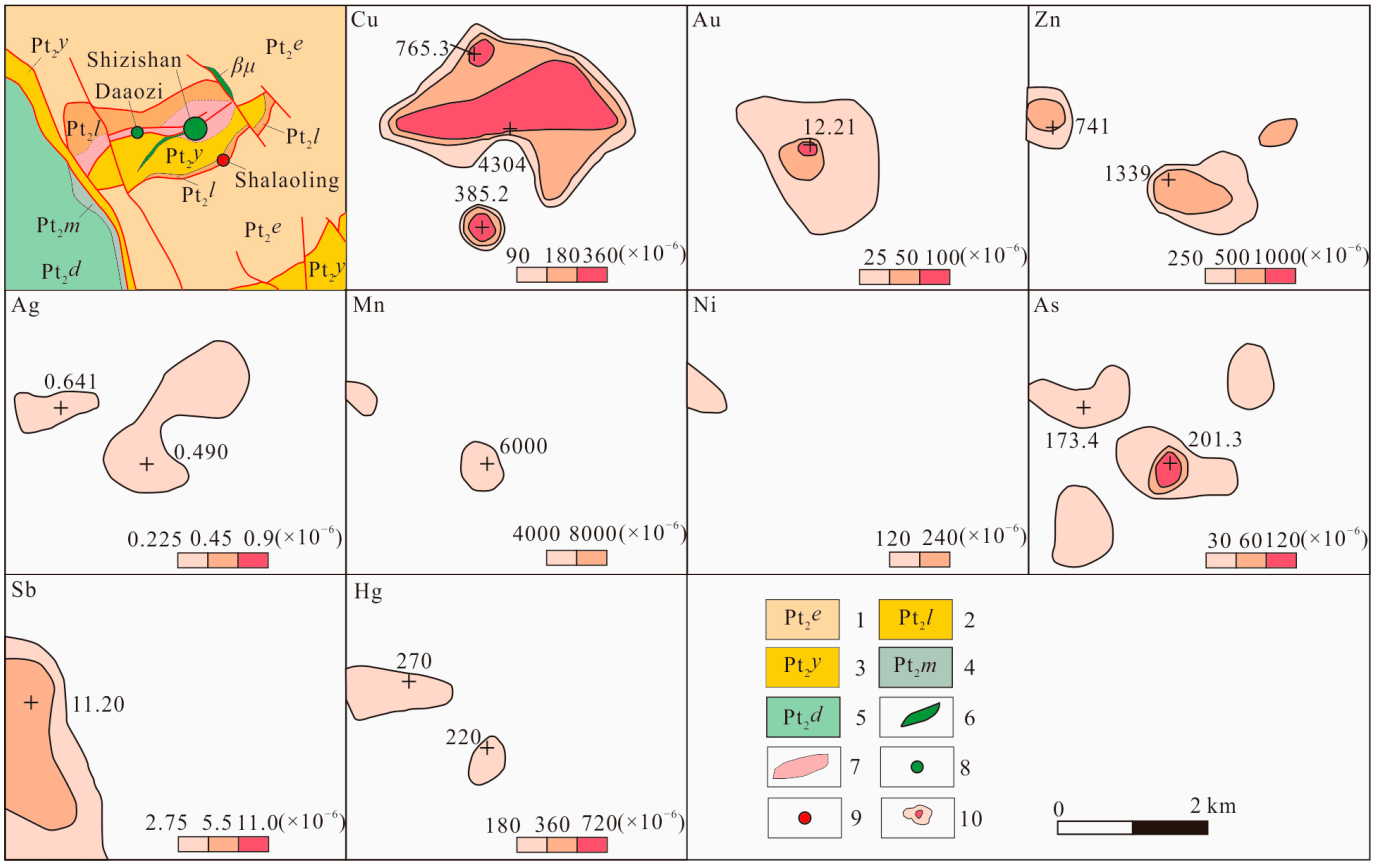


Figure 4. Integrated geochemical anomaly map of the SZS area in Yimen, Yunnan. Legend: 1—Etouchang Fm.; 2—Luoxue Fm.; 3—Yinmin Fm.; 4—Meidang Fm.; 5—Dalongkou Fm.; 6—Gabbro-diabase; 7—Copper ore body; 8—Copper occurrence; 9—Iron occurrence; 10—Single-element geochemical anomaly.

This anomaly is characterized by elevated Cu concentrations, pronounced zonation, and well-defined enrichment centers. The Cu values reach a maximum of 4304 ppm, with a mean value of 733.4 ppm and an anomaly contrast (anomaly-to-background) of 8.6. Spatially, the Au, Zn, and Ag anomalies coincide closely with the core of the Cu anomaly. By contrast, the As, Sb, and Hg anomalies are distributed along the western and southern peripheries, while Mn and Ni anomalies appear as sparse, localized features. R-mode cluster analysis (a multivariate statistical method) reveals two distinct elemental groupings: (1) a Cu–Pb–Ni–Mn–Bi cluster at a similarity level of 0.59, representing an inner horizontal zone of mineralization; and (2) an Ag–As–Sb–Au–Hg cluster at a similarity level of 0.42, defining a distal, outer horizontal halo.

3. Construction of the Prospecting Prediction Geological Model

3.1. Classification of Prospecting Prediction Deposit Types

Conventional models suggest that the DCT formed syngenetically during sedimentary diagenesis. Based on the presence of pyroclastic rocks with albite as the main component

within the sequences, some researchers previously classified them as marine volcanogenic exhalative-hydrothermal (VMS-like) deposits [59] or exhalative-brine sedimentary deposits [11]. However, contemporary studies indicate that these sodic rocks differ significantly from typical spilite–keratophyre assemblages and are instead the products of later hydrothermal metasomatism [20]. Most scholars now recognize the coupled importance of initial sedimentation and subsequent reworking, arguing that these deposits exhibit distinct epigenetic characteristics. For instance, Ran et al. [21] proposed a model involving "red-bed leaching, algal-controlled diagenetic mineralization, and tectonic enrichment". This model emphasizes the purple beds of the Yinmin Fm. as the primary source rocks and posits a sedimentary-diagenetic origin for the stratiform orebodies, with vein-type mineralization resulting from later geological reworking. Furthermore, Han et al. [14] introduced a more intricate framework involving "rift metallogenic settings, volcanic-hydrothermal sedimentation, tectonic reworking, and enrichment via deep-source magmatic superposition and groundwater circulation". This framework underscores the vital role of late-stage tectonic activity and deep-seated magmatic–hydrothermal overprinting in generating high-grade orebodies. Recent advancements have suggested that the DCT copper deposits are geologically comparable to those in the Central African Copper Belt, with mineralization driven by basin-scale brine circulation [18,60–63]. Specifically, Zhao et al. [17,18] posited that mineralization occurred during the later stages of basin evolution, triggered by the interaction between oxidized, metal-bearing brines derived from underlying red-bed sequences, and the host dolomites. In this framework, oxidized red beds, reduced strata, and evaporite sequences are recognized as the three fundamental lithostratigraphic components essential for ore formation [24]. Furthermore, Zhu et al. [20] argued that the Xikuangshan-, Dongchuan-, and Taoyuan- orebodies represent various components of a unified metallogenic system, formed through basinal brine metasomatism across diverse redox interfaces. Building upon these theories, this study emphasizes the primary controlling roles of redox interfaces and high-angle fault systems in the spatial localization of orebodies [64].

According to the established prospecting prediction classification scheme [2], the SZS copper deposit is categorized as a sedimentary-reformed type. Its genesis involved initial sedimentary geological processes, followed by non-magmatic hydrothermal activity and subsequent tectonic–magmatic hydrothermal overprinting and reworking. This classification is substantiated by three primary lines of evidence: (1) Mineralization within the Luoxue, Yinmin, and Etouchang formations is consistently restricted to specific horizons, reflecting regional lateral stability and underscoring the primary stratigraphic control on ore localization. (2) Copper mineralization exhibits unequivocal evidence of tectonic overprinting. Major fault structures, such as the F1 fault at the SZS deposit, controlled the occurrence of the primary orebodies (Figure 2). Hydrothermal alteration intensity decreases progressively with increasing distance from these faults, indicating their dual role as conduits for fluid migration and as favorable structural traps (detailed in Section 3.3). (3) The SZS deposit displays a complex thermal history, characterized by pervasive low-temperature alteration punctuated by localized high-temperature signatures. The presence of abundant vein-type orebodies (Figure 5a,b) and high-temperature hydrothermal fluid inclusions indicates a multi-stage mineralizing event. Regionally, the development of skarn minerals at depth in the nearby Fengshan and Dajianshan districts (Figure 5f) further suggests magmatic–hydrothermal overprinting (detailed in Section 3.4). This is corroborated by geophysical datasets, which suggest the existence of concealed intrusions beneath the SZS area (Figure 3b).

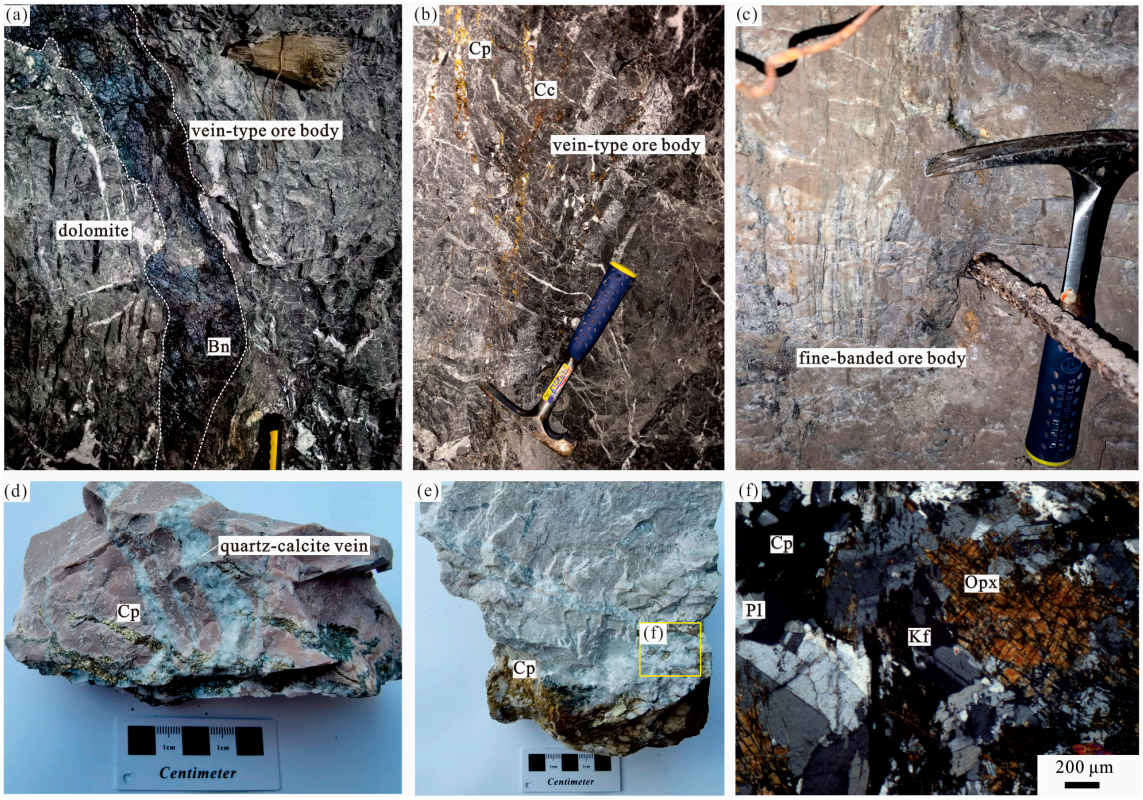


Figure 5. Macroscopic and microscopic characteristics of copper ores from the SZS area, Yimen, Yunnan: (**a**) hydrothermal vein-type copper ore from the SZS deposit, showing dolomite and Bornite (Bn); (**b**) vein structure in the SZS deposit, showing chalcopyrite (Cp) and chalcocite (Cc) occurring as stockworks and veinlets within dolomite; (**c**) banded copper ore from the SZS deposit; (**d**) vein-type copper ore from the Dajianshan deposit; (**e**) hydrothermal vein-type copper ore from the Dajianshan deposit, exhibiting skarn alteration; (**f**) skarn assemblage comprising K-feldspar (Kf), plagioclase (Pl), and orthopyroxene (Opx).

3.2. Metallogenic Geological Bodies

Metallogenic geological bodies are fundamental geological entities that provide both the material resources and the energy necessary for ore accumulation. They play a decisive role in determining the temporal and spatial distribution of mineral deposits as well as their genetic classification [2]. Given that the SZS copper deposit is classified as a sedimentary-reformed type, its metallogenic bodies are categorized based on two distinct evolutionary stages: (1) During the sedimentary-diagenetic stage, metallogenic geological bodies include the Proterozoic ore-bearing lithostratigraphic assemblages (specifically the Yinmin, Luoxue, and Etouchang formations) and the basin-margin fault structures that governed the primary depositional architecture of the rift. (2) During the subsequent tectonic–magmatic reworking stage, metallogenic geological bodies were manifested as regional fold–fault systems and deep-seated concealed (hidden) intrusive bodies. The former provided kinetic energy and pathways for fluid mobilization, while the latter served as the heat source and potentially contributed magmatic–hydrothermal components to the system.

3.3. Metallogenic Structures and Metallogenic Structural Planes

Metallogenic structures together with structural planes control the spatial location, morphology, and orientation of orebodies [2]. The SZS copper deposit is localized along the NE-trending SZS anticline and is hosted within the Yinmin, Luoxue, and Etouchang formations.

Metallogenic structures are geological structures that influence the formation and modification of ore deposits. They play a key role in controlling the material source, formation environment, and spatial distribution of these deposits. The structural framework of the district comprises several intersecting fault sets, including NE-, NW-, and nearly NS-trending systems. The primary metallogenic structural system is the NE-trending fold-and-fault network. This system is characterized by a series of tight folds and transpressional faults, locally associated with piercing structures (evaporitic salt diapirs), which are typically aligned with the NE-trending fault planes [65,66]. The principal ore-hosting structures include the hinge zones of the NE-trending anticlines, bedding-parallel (inter-stratal) detachment zones, and derivative secondary extensional faults (Figure 2b,c). By contrast, the NW-trending fault system developed post-mineralization, functioning as cross-cutting structures that offset and segmented the earlier NE-trending fracture network as well as the primary orebodies.

Metallogenic structural planes are explicit or implicit discontinuity surfaces within physical and chemical properties of rocks. These planes act as hosts for orebodies during mineralization and serve as spatial interfaces for the concentration and precipitation of ore-forming materials. The structural planes are categorized into primary and secondary types. The primary metallogenic structural planes consist primarily of lithological interfaces that function as redox boundaries. Key examples include the following: (i) the transitional beds between the argillaceous dolomitic limestone and the grayish–white dolomite of the Luoxue Fm.; (ii) the interbedded purple sandstone and slate with the light-colored feldspathic quartz sandstone of the Yinmin Fm.; and (iii) the interbedded black carbonaceous slate and dark gray dolomite of the Etouchang Fm. Within these sequences, carbonaceous slates and carbonaceous–argillaceous dolomites provided the biogenic reduced sulfur and organic matter that generated reducing fluids and established the redox interfaces essential for mineralization [33]. Evidence at depth suggests the existence of a second type of primary structural plane—magmatic intrusive interfaces. Recent exploration at the SZS deposit has identified copper-mineralized diabase dikes, where chalcopyrite and pyrite occur as disseminated clusters. These findings indicate a genetic link between these dikes and localized copper enrichment. Furthermore, the presence of magmatic–hydrothermal indicators, such as skarnization (Figure 5e) in the nearby Dajianshan deposit, further suggests that intrusive interfaces related to deep-seated magmatic systems acted as significant metallogenic structural planes during the later overprinting stages.

The secondary metallogenic structural planes are closely associated with the subsequent fold-related ore-controlling system. These include NE-trending fault planes, diapiric (piercing) structures, secondary faults generated during folding, inter-stratal (bedding-parallel) fracture zones, fold hinge zones, and structural dilation zones. These secondary planes served as high-permeability conduits for the migration of hydrothermal fluids and as the primary sites for mineral accumulation. Intense copper mineralization is concentrated within these fracture zones and their subsidiary joint and fissure networks. These structural planes are further characterized by pervasive wall–rock alteration, most notably intense silicification and chloritization, marking them as the zones of most vigorous hydrothermal activity and ore-fluid interaction.

The coupling of these favorable stratigraphic interfaces and structural systems, acting simultaneously as lithological discontinuities and physicochemical interfaces, constitutes a highly effective assemblage of metallogenic structural planes for large-scale copper accumulation.

3.4. Metallogenic Characteristics Markers

Metallogenic characteristic markers represent a series of geological indicators that can precisely delineate the occurrence positions of orebodies and hold pivotal importance for prospecting prediction. They constitute the primary evidence for delineating undiscovered and concealed orebodies. Such markers mainly encompass macroscopic orebody features, mineralogical attributes, metallogenic alteration halos, metallogenic epochs, transitional indicators of metallogenic physicochemical conditions, and the precipitation mechanisms of ore-forming materials [2].

3.4.1. Macroscopic Morphological Characteristics of Orebodies

The SZS copper deposit is characterized by multi-level mineralization, encompassing both stratiform and vein-type orebodies. The vein-type orebodies are primarily hosted within networks of extensional and transtensional fissures. By contrast, stratiform and stratabound orebodies are predominantly found within three distinct lithologies, the blue–gray stromatolitic (algal) dolomite of the lower Luoxue Fm., the purple sandstone and slate of the Yinmin Fm., and the black carbonaceous–argillaceous and arenaceous dolomite of the Etouchang Fm. [67].

(1) The primary mineralized zones are hosted within the blue–gray dolomite of the Luoxue Fm. These orebodies are localized within the hinge zones of the SZS anticline, demonstrating rigorous structural control. Their plunge is concordant with the anticlinal axis, descending steeply toward the northeast. Morphologically, the orebody margins are typically serrated or embayed. A defining characteristic of these orebodies is their limited strike length relative to their significant thickness and downdip extension. The downdip continuity often exceeds the strike length by a factor of >3.5, resulting in a distinct columnar or pipe-like geometry. Copper grades within these zones range from 0.52% to 1.77% (Figure 2c). (2) The orebodies hosted within the argillaceous dolomitic limestone and grayish–white dolomite of the transitional beds between the Luoxue and Yinmin formations are continuously distributed along the bedding. These orebodies are folded due to tectonic stress, appearing ribbon-like in plan view and corrugated slab-like in spatial morphology (Figure 2b). They are large in scale, with extensive strike and down-dip continuity, but remain relatively thin, with an average copper grade of 0.83%. (3) Moreover, orebodies hosted in the interbedded black carbonaceous slate and dark-gray thick-bedded dolomite of the Etouchang Fm. exhibit strong but uneven mineralization. These are currently identified only between the F5 and F6 faults, featuring a strike length of less than 50 m, an average thickness of 18.6 m, and copper grades ranging from 0.58% to 1.60%. (4) Furthermore, the orebodies are hosted within the light-colored, medium-to-thick bedded feldspathic quartz sandstone, interbedded with purple sandstone and slate of the Yinmin Fm. These orebodies are stratiform in nature and display consistency with the strike of the strata. These orebodies are smaller in scale but strongly mineralized, with a strike length of approximately 180 m, an average thickness of 3.9 m, and an average copper grade of 0.89%. Although their down-dip extension reaches 660 m, these orebodies thin noticeably at depth (Figure 2c).

3.4.2. Ore and Mineral Paragenesis

The ore textures of the SZS copper deposit include euhedral–subhedral granular, anhedral granular, replacement, inclusion, and brecciated-cemented textures. Ore structures commonly manifest as laminated, banded, vein-like, stockwork, densely disseminated, or spotted forms (Figure 2a–c). Bornite and chalcopyrite are frequently observed embedded along bedding planes and adjacent to fissures (Figure 2a). The primary sulfide assemblage is dominated by chalcopyrite, bornite, and pyrite, with accessory minerals including chal-

cocite, galena, and sphalerite. Gangue minerals consist primarily of dolomite, calcite, and quartz. Vertically, the mineral assemblage displays a distinct zonal progression from the surface to the deeper parts of the system. This transition begins with an oxidation zone (malachite + azurite + limonite), transitioning to a chalcopyrite + bornite assemblage in the shallower levels, and finally to a chalcopyrite + bornite + chalcocite + molybdenite (minor) association at depth. This progression indicates a trend toward medium-to-high temperature mineral assemblages in the deeper portions of the deposit.

3.4.3. Wall–Rock Alteration Characteristics

Wall–rock alteration in the study area is dominated by medium- to low-temperature assemblages, including bleaching, dolomitization, calcitization, silicification, sericitization, and chloritization [68]. Among these, silicification, dolomite recrystallization, and bleaching are the most closely associated processes with copper mineralization. The spatial relationship between wall–rock alteration and ore-controlling faults is well-defined, with alteration intensity decreasing progressively away from the fault planes [33]. Recent exploration data indicate the presence of skarnization and intense silicification, characteristic of high-temperature magmatic–hydrothermal activity in the deeper portions of the Yimen area. Specifically, tremolite–actinolite skarn copper orebodies have been identified in the twelfth-level tunnel of the Fengshan deposit. Furthermore, skarn-type mineralization has been documented in the deep-seated zones of the Dajianshan copper deposit, reflecting the significant role of magmatic overprinting and hydrothermal reworking in the regional metallogenic process [57].

3.4.4. Metallogenic Chronology

The metallogenic chronology of the SZS deposit is characterized by distinct mineralization episodes. Re–Os isotopic dating of vein-type copper ores within the Luoxue Fm. yielded three mineralization ages: 1755 ± 220 Ma, 1538 ± 130 Ma, and 449.4 ± 4.7 Ma [69]. Among these, the mineralization age of 1538 ± 130 Ma is interpreted as the primary tectonic-hydrothermal event associated with salt diapirism. Moreover, Ding et al. [33] reported a significant tectonic reworking mineralization age of 1405 ± 96 Ma. Previous research indicates that the DCT copper deposits are the product of multi-stage mineralization. The existing geochronological record contains significant uncertainties and wide-ranging data, fueling an ongoing debate regarding the precise timing of ore formation (Table S1). Nevertheless, a substantial body of data suggests that mineralization events primarily cluster around ~1.7, ~1.5, and ~0.8 Ga [12,19,33,69–74]. These age clusters are widely interpreted to represent: (i) the primary metallogenic event, (ii) a subsequent hydrothermal overprint related to mafic magmatism, and (iii) a later tectono-magmatic overprinting event, respectively [73].

3.4.5. Fluid Inclusion Characteristics

Fluid inclusion analysis of the SZS copper deposit reveals significant variations in homogenization temperatures (T_h) and salinities, indicating the presence of two distinct fluid systems (Figure 6d,e). The first system is characterized by low-to-medium temperature and medium-to-high salinity H_2O–NaCl fluids, which occur predominantly as liquid-rich and gas-rich inclusions. Homogenization temperatures range between 100 and 300 °C, with salinities of 12.5%–23.2% $NaCl_{eqv}$, and trapping pressures below 10 MPa. These parameters are consistent with a shallow, heated basinal brine origin [15]. Comparatively, the second system comprises high-temperature, high-salinity H_2O–NaCl fluids. This system is dominated by multiphase fluid inclusions, containing daughter minerals, predominantly halite, coexisting with liquid-rich and gas-rich inclusions. Homogenization temperatures range from 300 to 600 °C, while salinities reach 40%–70% $NaCl_{eqv}$, with fluid densities

between 1.10 and 1.20 g cm^{-3}. The coexistence of high-salinity multiphase inclusions alongside vapor-rich inclusions signifies fluid boiling or immiscibility. These characteristics reflect the overprinting of the system by deep-seated hydrothermal fluids likely derived from mafic intrusions [23].

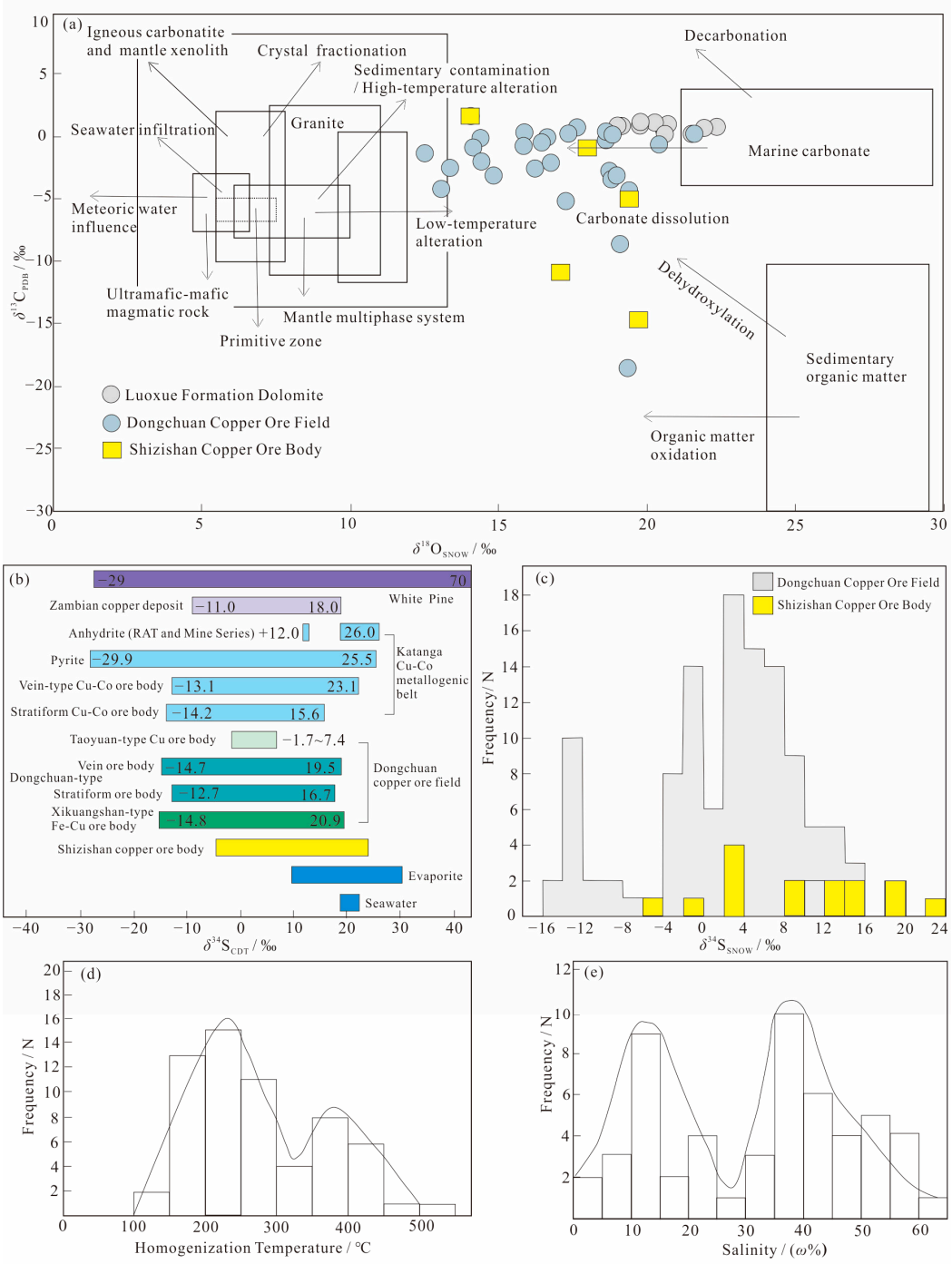


Figure 6. Stable isotope and fluid inclusion characteristics of the SZS copper deposit: (**a**) carbon and oxygen isotopes composition diagram; (**b**,**c**) histogram and distribution plot of sulfur isotope compositions; (**d**) histogram of fluid inclusion homogenization temperatures; and (**e**) histogram of fluid inclusion salinities. Data sources: [16,19,23,69,75–79] and references therein.

Carbon and oxygen isotope analyses yield $\delta^{18}O_{SMOW}$ values ranging from 14.07‰ to 19.25‰ (average 17.07‰) and $\delta^{13}C_{PDB}$ values between −10.51‰ and 0.39‰ (average −4.12‰). These results suggest that the ore-forming fluids were predominantly sourced

from formation water and brines generated through the dissolution of evaporites. The carbon source was predominantly sourced from marine carbonates. However, the lower $\delta^{13}C_{PDB}$ values likely reflect the oxidation and decarboxylation of organic matter, suggesting that organic material was actively involved in the mineralizing process [23,75] (Figure 6c). Spatially, a stratigraphic trend was observed from the Yinmin Fm. upward through the Luoxue and Etouchang (Heishan) formations, characterized by a progressive increase in $\delta^{18}O$ and a concomitant decrease in $\delta^{13}C$ [75].

Sulfur isotope signatures exhibit significant variability, with $\delta^{34}S$ values ranging from −4.37‰ to 23.40‰ (average 9.30‰) [68,76] (Figure 6d,e). This wide distribution suggests that the ore-forming sulfur was primarily sourced from the reduction of seawater sulfates, with a minor contribution from magmatic-derived sulfur.

3.4.6. Precipitation of Metal Elements

Previous studies have demonstrated that copper is transported in ore-forming fluids predominantly as chloride complexes (e.g., $CuCl_2^-$, $CuCl_3^{2-}$) [79]. The reduction in metals in fluids constitutes the primary mechanism driving the precipitation of metal sulfides during sedimentary and early diagenetic processes. Mineral precipitation is governed by the coupled influence of Eh and pH. The overall Eh–pH stability field for iron–copper sulfide precipitation extends across Eh values from approximately −0.8 to +0.379 V and pH values from 0 to 11.486 [79] (Figure 7). As the Eh decreases and pH increases, reflecting a transition from an acidic, relatively oxidizing fluid to an alkaline, relatively reducing fluid, the mineral assemblage precipitates in an ordered sequence of Pyrite → Chalcopyrite → Bornite → Chalcocite. With the decrease in temperature (488 K → 410 K, corresponding to the mineralization temperature of approximately 137 °C to 215 °C), the Eh stability range of pyrite and chalcopyrite contracts slightly, whereas the pH stability range of chalcopyrite and porphyrite broadens significantly toward alkalinity; however, this does not alter the previously established precipitation sequence (Figure 7).

Ore-forming stage	Sedimentary and early diagenetic processes	Tectonic-hydrothermal reworking process
Mineralization age	~1740–1680 Ma	Main reworking ~860–720 Ma; local early reworking at ~1450 Ma recorded
Tectonic setting	Mesoproterozoic continental rift basin (Kangdian Rift); restricted platform-lagoon facies	Neoproterozoic Jinning orogeny; compression-extension transition, fault-controlled
Ore occurrence	Stratiform, stratabound, concordant with bedding; mainly hosted in Luoxue Formation dolostone	Veins, veinlets, lenticular, cross-cutting; distributed along faults, fractures, and unconformities
Ore texture & structure	Fine-grained, framboidal, laminated; dominantly syngenetic sedimentary fabrics	Medium-coarse grained, metasomatic relict, veined; dominantly hydrothermal filling-metasomatic fabrics
Primary mineral assemblage	Chalcopyrite, bornite, pyrite, and chalcocite	Chalcopyrite, bornite, pyrite, and chalcocite; with tetrahedrite, tennantite, and other complex sulfides
Homogenization temperature	109 °C – 249 °C; basinal brine, low-temperature hydrothermal	115 °C – 310 °C, some are 318 °C – 550 °C (local spot data); low-moderate/ high temperature hydrothermal
Fluid salinity	1.66 – 20.22 wt% $NaCl_{eqv}$; basinal brine dominant	19.10 – 40.00 wt% $NaCl_{eqv}$, some are 35 – 63 wt% $NaCl_{eqv}$ (local spot data); high-salinity fluids well developed
Mineralization mechanism	Syngenetic sedimentary-diagenetic enrichment; organic matter reduction + sulfate reduction driving sulfidation	Tectonically driven fluid migration + water-rock reaction; fluid mixing, boiling, cooling trigger sulfide precipitation
Sulfide evolution sequence	Closed reducing system: Pyrite → Chalcopyrite → Bornite → Chalcocite; unidirectional evolution with Eh↓, pH↑, T↓	Open hydrothermal system: reverse metasomatism possible; hydrothermal fluids may metasomatize early sulfides
Eh–pH stability field of the mineral	The thermodynamic Eh-pH stable ranges of pyrite, chalcopyrite, and bornite (488 K → 410 K): Pyrite: Eh -0.075~0.379, pH 0~2.525 / Eh -0.069~0.333, pH 0~2.668; Chalcopyrite: Eh -0.589~0.094, pH 0.777~8.099 / Eh -0.595~0.080, pH 0.844~9.755; Bornite: Eh -0.800~-0.589, pH 6.087~9.90 / Eh -0.800~-0.595, pH 7.305~11.486. The dominant fields Eh-pH phase diagram of various elements and minerals in hot water solution (T=488 K)	

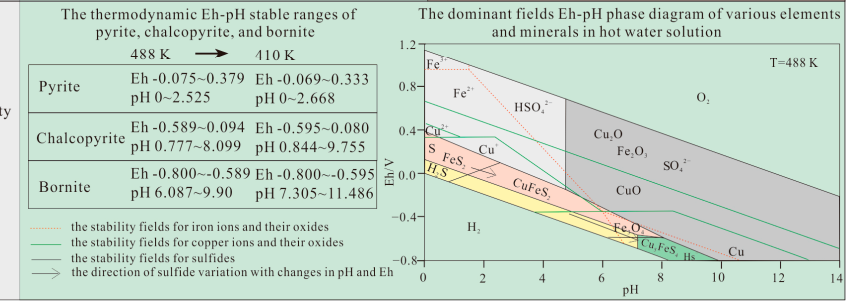


Figure 7. Comparison of two-stage mineralization characteristics for the DCT, and the Eh–pH stability phase diagram of sulfides. Data sources: [15,16,23,29,76–79] and references therein.

3.5. "Three-in-One" (Trinity) Prospecting Prediction Geological Model

During the Paleoproterozoic, the western margin of the Yangtze Block transitioned into a passive continental margin following the fragmentation of the Columbia supercontinent [44,45]. The subsequent rifting and subsidence of the crystalline basement facilitated the development of major NS-trending deep-seated faults, which governed the architecture of the Kunyang Rift and Yimen fault-bounded basins. Within these basins, a transgressive sedimentary succession developed, encompassing the Yinmin, Luoxue, and Etouchang formations, transitioning from basal siliciclastic sandstone–shale to dolomitic carbonates and black carbonaceous shales. This initial sedimentary-diagenetic phase resulted in the primary enrichment of ore-forming elements, specifically copper and iron. The oxidized red-bed sequences of the Yinmin Fm. and the underlying basement rocks were identified as the critical metal source beds for these copper deposits [17–19,22].

Sedimentary and early diagenetic processes, including compaction, dissolution of evaporites, salt diapirism, and contemporaneous mafic intrusions provided the primary thermal and tectonic driving forces for large-scale basinal fluid migration (Figure 8). These processes facilitated the generation of formation waters and basin brines that leached and extracted metals, notably copper, from the Proterozoic source beds to form oxidized, metal-bearing brines [24,79–81]. These fluids ascended along high-angle faults, traversed major lithological redox boundaries, and infiltrated reducing lithologies such as the Luoxue Fm. dolomites and Etouchang Fm. carbonaceous slates. Mixing of these oxidized brines with reducing fluids induced a rapid decline in temperature, oxygen fugacity, and sulfur fugacity, promoting the precipitation of copper sulfides and establishing the characteristic multi-level stratigraphic control observed in the district [68]. Organic-rich strata, including carbonaceous slates and stromatolitic dolomites, functioned both as chemical traps (redox interfaces) and as critical sources of biogenic reduced sulfur [29]. As the mineralizing fluids cooled and reached equilibrium, a distinct vertical zonation of minerals emerged, extending upward from the Yinmin Fm. through to the Etouchang Fm. This progression is expressed in a paragenetic sequence, transitioning from hematite (specularite) to chalcocite, then bornite, followed by chalcopyrite, and finally pyrite [23,82].

The tectonic-hydrothermal reworking process was initiated by the Neoproterozoic Jinning Orogeny, which induced regional folding and uplift and was characterized by intense compressional deformation that resulted in a series of NE-trending fold-and-thrust systems, most notably the SZS anticlinorium. During this period, deep-seated faults underwent extensive reactivation. This reactivation was accompanied by significant magmatic activity along the fault zones, which provided the high heat flow and thermal energy (both tectonic and magmatic-hydrothermal) necessary to catalyze the system. These processes generated high-temperature fluids that facilitated the remobilization and migration of ore-forming materials from the pre-existing Proterozoic stratiform copper source beds. As these mineralizing fluids ascended into shallower, dilational structural domains, they experienced rapid pressure reduction and phase separation (boiling), which triggered the precipitation and concentrated enrichment of ore minerals (Figure 7). This mechanism is responsible for both the superimposed enrichment and the ultimate metallogenic emplacement of the high-grade orebodies [15,82–85]. The spatial distribution of the broader ore fields was primarily controlled by regional NS- and NE-trending structures, such as the Lüzhijiang and Yimen faults. At the local scale, secondary longitudinal faults within anticlinal cores and piercing (diapiric) structures served as high-permeability pathways for hydrothermal fluid migration. The ultimate geometry and location of the orebodies were determined by shallow structural traps, including fold hinges, inter-stratal detachment zones, and extensional joint networks. Within the fold cores, mineralization manifested as structurally controlled, columnar orebodies. By contrast, the stratiform and lenticular

orebodies localized along the fold limbs resulted from compressional drag effects and bedding-parallel slip during the peak of the orogenic deformation.

During the post-mineralization stage, the region was subjected to near NS-oriented compressional stress associated with the Caledonian orogeny. This tectonic regime resulted in the development of a series of NWW- to nearly EW-trending fault systems across the study area. These late-stage structures significantly offset the deep-seated orebodies. Specifically, the footwall segments exhibit a horizontal displacement of approximately 80–120 m toward the southwest in plan view and a corresponding downdip displacement of 80–120 m in cross-section view [33].

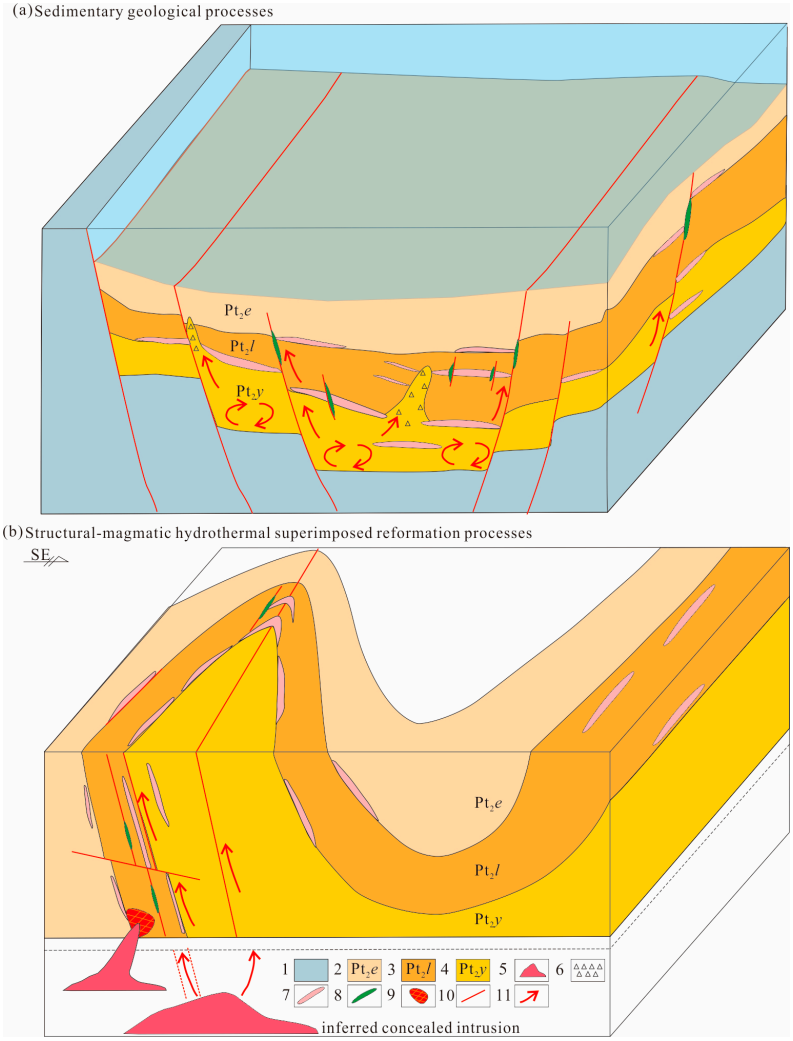


Figure 8. Geological model for prospecting prediction for the SZS copper deposit: Legend: 1—Basement rocks; 2—Etouchang Fm.; 3—Luoxue Fm.; 4—Yinmin Fm.; 5—Concealed intrusion; 6—Breccia; 7—Stratiform copper ore body; 8—Vein-type copper ore body; 9—Skarn alteration; 10—Fault; 11—Hydrothermal fluid flow direction.

4. Comprehensive Information Model for Prospecting Prediction

This model integrates geophysical and geochemical datasets to establish a comprehensive predictive framework for the SZS copper deposit.

Geophysical characteristics: Statistical analysis of petrophysical parameters reveals that the dolomite within the SZS mining area exhibits the highest resistivity (typically >3000 Ω m) and the lowest polarizability (typically <2%). Conversely, carbonaceous slate is characterized by low resistivity (<200 Ω m) and high polarizability (>10%). Copper ore

demonstrates the lowest resistivity (<100 Ω m) and relatively high polarizability (>5%). Mineralized rocks show higher resistivity than massive copper ore, with a broader range of variation and relatively low polarizability. In general, when carbonaceous slate is excluded, the polarizability of copper ore is approximately five times higher than that of the surrounding lithologies, while the resistivity of the host rocks is 10 to 50 times greater than that of the ore. This confirms that the copper mineralization is characterized by a "low resistivity, high polarizability" signature. The pronounced contrast in resistivity and polarizability between the ore bodies and the surrounding host rocks makes electrical methods highly effective tools for delineation. Specifically, the Luoxue Fm. acts as a high-resistivity, low-polarization background, within which the orebodies appear as distinct low-resistivity and high-polarization anomalies. Resistivity gradient zones and localized low-resistivity anomalies embedded within high-resistivity backgrounds constitute high-priority targets for mineral exploration. High-precision ground magnetic surveys are instrumental for delineating the lithological boundaries between the Etouchang and Luoxue formations, while electromagnetic (EM) anomalies provide diagnostic markers for identifying the Luoxue Fm. sequences, inter-stratal faults, and mineralized copper bodies. Regionally, the primary structural targets for "Dongchuan-type" mineralization are secondary fold belts situated adjacent to major fault systems, specifically at the intersections of anticlinal hinges with NW- and NE-trending faults. Copper mineralization is typically localized along the peripheries of low-amplitude gravity highs and within zones characterized by increasing magnetic field values relative to a negative background. Given that the Dongchuan Group generally displays relatively high magnetic intensities, 1:50,000-scale magnetic surveys are highly effective for mapping concealed stratigraphy and identifying NE-trending structural framework.

At the 1:50,000 scale, geochemical anomalies are primarily characterized by a Cu–Au–Zn–Ag elemental association, typically accompanied by As, Sb, Hg, Mn, and Ni anomalies. Horizontally, Cu, Mo, Bi, Co, and Mn serve as proximal indicator elements, whereas Pb and Ag anomalies act as distal (remote) indicators. Conversely, the vertical (axial) geochemical zonation sequence for the copper mineralization is defined as Mn–Ba–Ag–Cu–Zn–Co–Pb–Bi–Mo. Within this framework, Mn, Ba, and Ag represent the supra-ore (frontal) halo elements; Ag, Cu, Zn, Co, and Pb constitute the proximal (ore-stage) halo elements; and Bi and Mo function as the high-temperature sub-ore (tail) halo elements [77].

5. Prospecting Directions and Target Delineation

(1) The DCT copper deposits are characterized by multi-horizon mineralization, wherein the redox interface serves as the primary ore-controlling structural plane. The SZS deposit, specifically, comprises five distinct ore-bearing stratigraphic horizons. Historically, systematic explorations in the peripheral areas of the mining district have focused almost exclusively on orebodies within the Luoxue Fm. However, owing to the steep inclination of the orebodies (Figure 2c), a significant number of previous drill holes failed to penetrate the critical contact boundary between the Luoxue and Yinmin formations. Consequently, future exploration must prioritize these underexplored horizons. By systematically mapping the distribution of lateral copper-bearing veins and clarifying the architecture of the fluid feeder systems (metallogenic supply systems), there is high potential for significant breakthroughs in identifying mineralization within these new horizons [20].

(2) The DCT copper deposits typically exhibit low primary ore grades, often ranging between 0.3% and 0.4%. However, subsequent tectono-magmatic hydrothermal overprinting can facilitate the development of high-grade, massive orebodies (>1%) with substantial economic significance [37,86,87]. For instance, although the average copper grade at the

SZS deposit is approximately 0.4%, localized zones influenced by structural overprinting can exceed 2.0%. The primary mineralizing architecture in the region is defined by a NE-trending "fold-and-fault" structural framework. Anticlinal hinges and their intersections with NE-trending faults are particularly favorable areas for discovering high-grade ore. Consequently, deep-seated exploration and prospecting in covered areas should transition from a conventional "stratabound" exploration paradigm to one that prioritizes tectono-magmatic hydrothermal overprinting and superimposition processes. Future efforts should focus specifically on identifying concealed magmatic intrusions and structural superposition zones situated along major NE-trending fault systems.

(3) Most of the known deposits in the district are concentrated along the linear gradient zones of residual Bouguer gravity anomalies and proximal to moderate-to-high magnetic anomalies. This spatial correlation underscores the fundamental control exerted by syn-metallogenic fault systems on ore localization. To leverage this relationship in target delineation, advanced potential field processing techniques were employed in this study. Boundary enhancement algorithms were applied for the edge direction of gravity anomalies (Figure 9b), while regularized filtering was used to isolate and extract residual magnetic anomalies. By integrating these two datasets, co-located zones characterized by both high gravity gradients and positive magnetic anomalies were identified. These overlapping geophysical signatures provide a robust, data-driven basis for narrowing down high-priority exploration targets (Figure 9c).

(4) By combining field geological surveys with an integrated analysis of legacy and new geophysical and geochemical datasets, this study defines a "stratigraphy + structure + concealed intrusions" framework as the primary multi-parametric criterion for exploration targeting. By applying these criteria to the covered peripheral zones and deep-seated horizons of the SZS district, and incorporating high-resolution geophysical interpretations, three high-priority target areas were delineated (Figure 9, Table S2). These targets are characterized by a high metallogenic potential for the discovery of concealed, high-grade orebodies at depth.

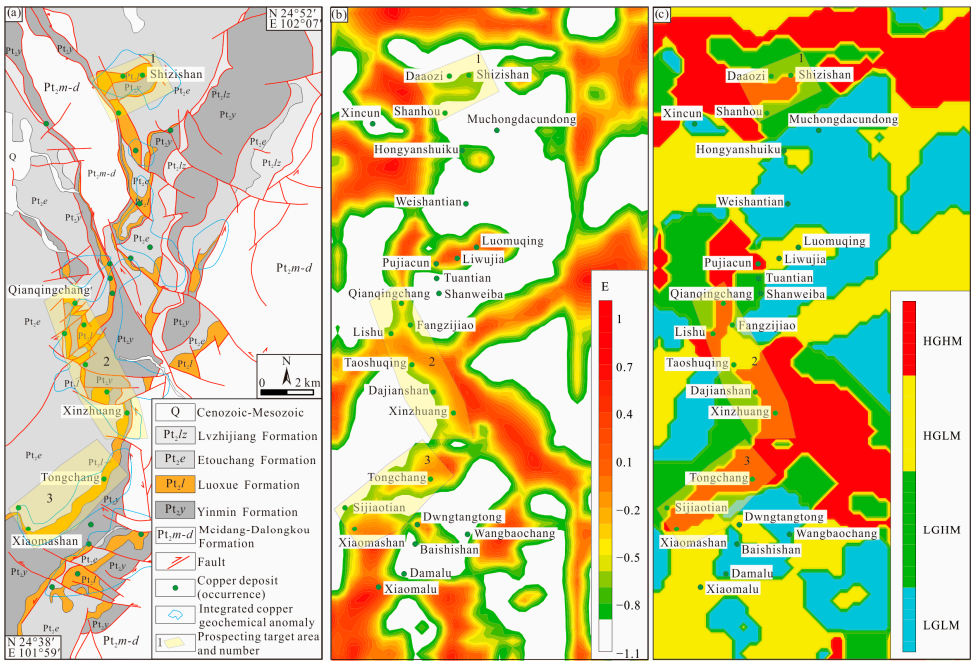


Figure 9. Integrated mineral exploration prediction map for the SZS area, Yimen, Yunnan: (**a**) mineral prediction map; (**b**) edge-enhanced Bouguer gravity anomaly; and (**c**) correlation analysis results of gravity and magnetic anomalies.

6. Conclusions

(1) The SZS copper deposit is characterized by multi-episodic mineralization and is classified as a sedimentary-reformed deposit. Its metallogenic evolution unfolded three distinct stages: (i) primary sedimentary-diagenetic processes; (ii) non-magmatic hydrothermal activity; and (iii) subsequent tectonic-magmatic hydrothermal overprinting and reworking.

(2) A comprehensive "Three-in-One" (Trinity) prospecting prediction model was established for the SZS deposit. Within this framework, the metallogenic geological bodies comprise Proterozoic ore-bearing stratigraphic associations, basin-margin faults, and Neoproterozoic fold–fault systems associated with deep-seated concealed intrusions. The metallogenic structural planes are defined by primary lithological redox interfaces and secondary surfaces within the fold–fault structural systems. The metallogenic characteristic indicators are primarily represented by macroscopic hydrothermal alteration assemblages, including pervasive bleaching, dolomitization, and silicification.

(3) Future exploration in covered and deep-seated areas should prioritize regions of intense tectono-magmatic overprinting and structural reworking. Specifically, targeting efforts should focus on the spatial convergence of favorable lithostratigraphic horizons, concealed magmatic intrusions, and NE-trending structural systems.

(4) An integrated, multi-parametric prospecting model was established for the SZS copper deposit. By applying a screening framework based on "stratigraphy + structure + concealed intrusions" and synthesizing integrated geophysical and geochemical datasets, three high-priority exploration targets were delineated. These findings provide a robust scientific basis for the deployment of subsequent deep-resource exploration and drilling programs within the Yimen area.

Supplementary Materials: The following supporting information can be downloaded at: https://www.mdpi.com/article/10.3390/min16080833/s1, Table S1: Summary of the published isotope dating from Dongchuan-type copper deposits in Kangdian region [12,19,23,33,69–74]; Table S2: A list of prospecting target areas for the Shizisan area, Yimen, Yunnan [88].

Author Contributions: Data treatment and writing original draft, X.Z., J.W. and G.C.; review and editing, H.C., B.Y., X.W. and Z.P.; supervision and funding acquisition, X.Z. All authors have read and agreed to the published version of the manuscript.

Funding: This research was funded by the National Key Research and Development Program Project (Grant No. 2023YFC2906405), the Yunnan Province Major Science and Technology Special Project (Grant No. 202402AB080006-2), the China Geological Survey Program (Grant Nos. DD20230355 and DD202602109902), and the Natural Science Foundation of Henan Province (Grant No. 252300421472).

Data Availability Statement: The data that support the findings of this study are available on request from the corresponding author.

Acknowledgments: We sincerely appreciate the thoughtful comments provided by the reviewers on our manuscript.

Conflicts of Interest: The authors declare that there are no conflicts of interest. XiaTao WU is an employee of Yunnan Copper Mineral Resources Exploration and Development Co., Ltd. The paper reflects the views of the scientists and not the company.

Abbreviations

The following abbreviations are used in this manuscript:

MGBT	Metallogenic geological body theory
DCT	"Dongchuan-type" copper deposits
Fm.	Formation
SZS	Shizishan

References

1. Lv, Z.C.; Chen, H.; Mi, K.F.; Zhang, B.L.; Xie, Y.Q.; Pang, Z.S.; Cheng, Z.Z.; Xue, J.L.; Gong, F.Y.; Duan, B.; et al. The theory and method of ore prospecting prediction for exploration area: Case studies of the Lala copper deposit in Sichuan, Muhu–Maerkantu manganese ore deposit in Xinjiang and Aonaodaba tin-polymetallic deposit in Inner Mongolia. *J. Geomech.* **2022**, *28*, 842−865. (In Chinese with English abstract)
2. Ye, T.Z.; Lv, Z.C.; Pang, Z.S. *Inclusion of Prospecting Prediction Theory and Method in Exploration Area (General Theory)*; Geological Publishing House: Beijing, China, 2014; pp. 1–703. (In Chinese)
3. White, N.C.; Hedenquist, J.W. Epithermal gold deposits: Styles, characteristics and exploration. *SEG Newsl.* **1995**, *23*, 9–13.
4. Singer, D.A.; Menzie, W.D. *Quantitative Mineral Resource Assessments: An Integrated Approach*; Oxford University Press: New York, NY, USA, 2010.
5. Zhao, P.D. Quantitative mineral prediction and deep mineral exploration. *Earth Sci. Front.* **2007**, *14*, 1–10. (In Chinese with English abstract). [CrossRef]
6. Pang, Z.S.; Xue, J.L.; Cheng, Z.Z.; Chen, H.; Zhang, X.F.; Jia, R.Y.; Wei, H.T.; Zuo, Q.C.; Lei, X.L.; Zhang, Z.H.; et al. Application of the prospecting prediction theory and method of metallogenic geological body in ore-prospecting prediction. *Geol. Bull. China* **2023**, *42*, 883–894. (In Chinese with English abstract)
7. Chen, H.; Lin, L.J.; Pang, Z.S.; Cheng, Z.Z.; Xue, J.L.; Tao, W.; Ma, Y.X.; Gong, L.M.; Shen, H.T. Construction and demonstration of an ore prospecting model for the Lala copper deposit in Huili, Sichuan. *Earth Sci. Front.* **2021**, *28*, 309–327. (In Chinese with English abstract)
8. Hou, L.; Ding, J.; Deng, J.; Peng, H.J. Geology, Geochronology, and Geochemistry of the Yinachang Fe–Cu–Au–REE Deposit of the Kangdian Region of SW China: Evidence for a Paleo–Mesoproterozoic Tectono-Magmatic Event and Associated IOCG Systems in the Western Yangtze Block. *J. Asian Earth Sci.* **2015**, *103*, 129–149. [CrossRef]
9. Zhao, X.F.; Zhou, M.F. Fe-Cu deposits in the Kangdian region, SW China: A Proterozoic IOCG (iron-oxide-copper-gold) metallogenic province. *Miner. Depos.* **2011**, *46*, 731–747. [CrossRef]
10. Zhang, X.L.; Liu, H.T. *Report on the Strategic Mineral Prospectivity Survey of the Yimen Area, Yunnan Province*; Yunnan Provincial Bureau of Nonferrous Metals Geology: Yunnan, China, 2013; pp. 1–433. (In Chinese)
11. Gong, L.; He, Y.T.; Chen, T.Y. *Proterozoic Rift Type Copper Deposits in Dongchuan, Yunnan Province*; Metallurgical Industry Press: Beijing, China, 1996. (In Chinese with English abstract)
12. Huang, X.W.; Zhao, X.F.; Qi, L.; Zhou, M.F. Re-Os and S isotopic constraints on the origins of two mineralization events at the Tangdan sedimentary rock-hosted stratiform Cu deposit, SW China. *Chem. Geol.* **2013**, *347*, 9–19. [CrossRef]
13. Cox, D.P.; Lindsey, D.A.; Singer, D.A.; Moring, B.C.; Diggles, M.F. *Sediment-Hosted Copper Deposits of the World: Deposit Models and Database*; Geological Survey: Reston, VA, USA, 2007.
14. Han, R.S.; Liu, C.Q.; Sun, K.X.; Ma, D.Y.; Li, Y. Composite poly-genesis of Yimen-type copper deposits. *Geotecton. Met.* **2000**, *24*, 146–154. (In Chinese with English abstract)
15. Li, Q.; Wang, L.; Mao, J.H.; Zuo, Q.H.; Meng, S.R. Research on the Fluid Inclusions of Shizishan Copper Deposit, Yunnan. *Geotecton. Met.* **2013**, *37*, 57–64. (In Chinese with English abstract)
16. Yang, Y.; Han, R.S.; Wang, L.; Li, B.; Hu, Y.D. Geochemical characteristics of basic intrusive rocks in Shizishan copper deposit Yimen Yunnan and its geological significance. *J. Mineral. Pet.* **2010**, *30*, 69–74. (In Chinese with English abstract)
17. Zhao, X.F.; Zhou, M.F.; Li, J.W.; Sun, M.; Gao, J.F.; Sun, W.H.; Yang, H.Y. Late Paleoproterozoic to early Mesoproterozoic Dongchuan Group in Yunnan, SW China: Implications for tectonic evolution of the Yangtze Block. *Precambrian Res.* **2010**, *182*, 57–69. [CrossRef]
18. Zhao, X.F.; Zhou, M.F.; Hitzman, M.W.; Li, J.W.; Bennett, M.; Meighan, C.; Anderson, E. Late Paleoproterozoic to Early Mesoproterozoic Tangdan sedimentary rock-hosted strata–bound copper deposit, Yunnan Province, Southwest China. *Econ. Geol.* **2012**, *107*, 357–375. [CrossRef]
19. Ran, C.Y.; Wu, P. Discussions on the Metallogeny of the Dongchuan-Yimen Type Copper Deposits, Yunnan, China. *Geotecton. Met.* **2014**, *38*, 848–854. (In Chinese with English abstract)
20. Zhu, X.Y.; Zhang, X.; Jiang, C.H.; Wang, H. The epigenetic origin and exploration significance of Dongchuan copper deposit, Yunnan. *Acta Mineral. Sin.* **2017**, *37*, 154–155. (In Chinese) [CrossRef]
21. Ruan, H.C.; Hua, R.M.; Ni, P. New approaching to the genesis of Dongchuan type copper deposits. *Contrib. Geol. Miner. Resour. Res.* **1988**, *3*, 9–22. (In Chinese with English abstract)
22. Hua, R.M. On the "sedimentation-transformation" genesis of the Dongchuan type stratiform copper deposits. *Miner. Depos.* **1989**, *8*, 3–13. (In Chinese with English abstract)
23. Zeng, R.G. Comparative Study on Mineralization between Yinmin Copper Deposit in Yunnan Dongchuan and Luiswishi Copper-Cobalt Deposit in Democratic Republic of the Congo. Master's Thesis, Kunming University of Science and Technology, Kunming, China, 2021. (In Chinese with English abstract)

24. Hitzman, M.W.; Kirkham, R.; Broughton, D.; Thorson, J.; Selley, D. The sediment-hosted stratiform copper ore system. *Econ. Geol.* **2005**, *100*, 609–642. [CrossRef]
25. Hitzman, M.W.; Broughton, D.; Selley, D.; Woodhead, J.; Wood, D.; Bull, A. The Central African Copperbelt: Diverse stratigraphic, structural, and temporal settings in the world's largest sedimentary copper district. *Econ. Geol.* **2012**, *16*, 487–514.
26. Hitzman, M.W.; Broughton, D.W. Discussion: "age of the Zambian copperbelt" by sillitoe et al. (2017) mineralium deposita. *Miner. Depos.* **2017**, *52*, 1273–1275. [CrossRef]
27. Hoggard, M.J.; Czarnota, K.; Richards, F.D.; Huston, D.L.; Jaques, A.L.; Ghelichkhan, S. Global distribution of sediment-hosted metals controlled by craton edge stability. *Nat. Geosci.* **2020**, *13*, 504–510. [CrossRef]
28. Igor Azeuda Ndonfack, K.; Yang, Z.M.; Zhang, J.L.; Whattam, S.A.; Xie, Y.L. Geology, geochemistry, and exploration of the Central African Copper- belt: A review. *Int. Geol. Rev.* **2025**, *67*, 1098–1131.
29. Yin, X.Q.; Lin, H.T.; Su, Z.K.; Zhao, X.F. Mineralization and subsequent overprint history of Dongchuan-type copper deposits: Constraints from in situ sulfur isotope of sulfides. *Miner. Depos.* **2021**, *40*, 34–52. (In Chinese with English abstract) [CrossRef]
30. Sillitoe, R.H.; Perelló, J.; Creaser, R.A.; Wilton, J.; Wilson, A.J.; Dawborn, D. Age of the Zambian copper belt. *Miner. Depos.* **2017**, *52*, 1245–1268. [CrossRef]
31. Perelló, J.; Sillitoe, R.H.; Yakubchuk, A.S.; Valencia, V.A.; Cornejo, P. Age and tectonic setting of the Udokan sediment-hosted copper-silver deposit, Transbaikalia, Russia. *Ore Geol. Rev.* **2017**, *86*, 856–866. [CrossRef]
32. Perelló, J.; Valencia, V.A.; Comejo, P.; Clifford, J.; Wilson, A.J.; Collins, G. Timing of sediment-hosted Cu-Ag mineralization in the Trans-Hudson orogen at Janice Lake, Wollaston Domain, Saskatchewan, Canada. *Miner. Depos.* **2019**, *54*, 81–100.
33. Ding, J.J.; Wang, L.; Ren, T.; Mao, J.H.; Zhao, D.; Zhu, E.Y.; Chen, X.L.; Jiang, Z.H.; Huang, Y.H. Ore-control Structures of Shizishan Copper Deposit in Yimen Country and Deep Prospecting. *Geotecton. Met.* **2020**, *44*, 1128–1142. (In Chinese with English abstract)
34. Zhou, J.W.; Jiang, X.S.; Wang, J.; Cui, X.Z.; Xiong, G.Q.; Lu, J.Z.; Liu, J.H.; Ma, M.Z. Opening time and filling pattern of the Neoproterozoic Kangdian Rift Basin, western Yangtze Continent, South China. *Sci. China Earth Sci.* **2013**, *56*, 1664–1676. [CrossRef]
35. Zhao, G.C.; Cawood, P.A. Precambrian geology of China. *Precambrian Res.* **2012**, *222–223*, 13–54. [CrossRef]
36. Wang, S.W.; Jiang, X.F.; Yang, B.; Sun, X.M.; Zhou, Q.; Guo, Y.; Wang, Z.Z.; Yang, B.; Liao, Z.W. The Proterozoic Tectonic Movement In Kangdian Area: Kunyang Intracontinental Rift, Mantle Plume and Its Metallogenesis. *Geol. Rev.* **2016**, *62*, 1353–1377. (In Chinese with English abstract)
37. Wu, P.; Zhang, S.B.; Zheng, Y.F.; Fu, B.; Liang, T. Amalgamation of South China into Rodinia during the Grenvillian accretionary orogeny: Geochemical evidence from Early Neoproterozoic igneous rocks in the northern margin of the South China Block. *Precambrian Res.* **2019**, *321*, 221–243. [CrossRef]
38. Liu, H.C.; Zi, J.W.; Cawood, P.A.; Gui, X.; Zhang, L.M. Reconstructing South China in the Mesoproterozoic and its role in the Nuna and Rodinia supercontinents. *Precambrian Res.* **2020**, *337*, 105558. [CrossRef]
39. Hu, P.Y.; Zhai, Q.G.; Wang, J.; Tang, Y.; Ren, G.M.; Zhu, Z.C.; Wang, W.; Wu, H. U–Pb zircon geochronology, geochemistry, and Sr–Nd–Hf–O isotopic study of Middle Neoproterozoic magmatic rocks in the Kangdian Rift, South China: Slab rollback and backarc extension at the northwestern edge of the Rodinia. *Precambrian Res.* **2020**, *347*, 105863. [CrossRef]
40. Hu, P.Y.; Zhai, Q.G.; Wang, J.; Tang, Y.; Ren, G.M. The Shimian ophiolite in the western Yangtze Block, SW China: Zircon SHRIMP U-Pb ages, geochemical and Hf-O isotopic characteristics, and tectonic implications. *Précambr. Res.* **2017**, *298*, 107–122. [CrossRef]
41. Du, B.; Yang, Z.A.; Yang, L.F.; Chen, Q.; Zhu, J.X.; Shi, K.X.; Lu, J. Zircon Hf isotopic mapping applied to the metal exploration of the Sanjiang tethyan orogenic belt, Southwestern China. *Appl. Sci.* **2022**, *12*, 4081. [CrossRef]
42. Wang, L.J.; Yu, J.H.; Griffin, W.L.; Reilly, S.Y.O. Early crustal evolution in the western Yangtze Block:Evidence from U-Pb and Lu-Hf isotopes on detrital zircons from sedimentary rocks. *Precambrian Res.* **2012**, *222*, 368–385. [CrossRef]
43. Cawood, P.A.; Zhao, G.C.; Yao, J.L.; Wang, W.; Xu, Y.J.; Wang, Y.J. Reconstructing South China in Phanerozoic and Precambrian supercontinents. *Earth Sci. Rev.* **2018**, *186*, 173–194. [CrossRef]
44. Wang, W.; Zhou, M.F. Provenance and tectonic setting of the Paleo- to mesoproterozoic Dongchuan group in the Southwestern Yangtze block, South China: Implication for the breakup of the supercontinent Columbia. *Tectonophysics* **2014**, *610*, 110–127. [CrossRef]
45. Wang, W.; Zhou, M.F.; Zhao, X.F.; Chen, W.T.; Yan, D.P. Late paleoproterozoic to mesoproterozoic rift successions in SW China: Implication for the Yangtze Block-North Australia-Northwest Laurentia connection in the Columbia supercontinent. *Sediment. Geol.* **2014**, *309*, 33–47. [CrossRef]
46. Lu, G.M.; Wang, W.; Cawood, P.A.; Ernst, R.E.; Raveggi, M.; Huang, S.F.; Xue, E.K. Late paleoproterozoic to early mesoproterozoic mafic magmatism in the SW Yangtze block: Mantle plumes associated with Nuna breakup? *J. Geophys. Res. Solid Earth* **2020**, *125*, e2019JB019260. [CrossRef]
47. Cui, X.Z.; Jiang, X.S.; Wang, J.; Wang, X.C.; Zhuo, J.W.; Deng, Q.; Liao, S.Y.; Wu, H.; Jiang, Z.F.; Wei, Y.A. Mid-Neoproterozoic diabase dykes from Xide in the western Yangtze Block, South China: New evidence for continental rifting related to the breakup of Rodinia supercontinent. *Précambr. Res.* **2015**, *268*, 339–356. [CrossRef]

48. Chen, W.T.; Zhou, M.F. Paragenesis, stable isotopes, and molybdenite Re-Os isotope age of the Lala iron-copper deposit, Southwest China. *Econ. Geol.* **2012**, *107*, 459–480. [CrossRef]
49. Su, Z.K.; Zhao, X.F.; Li, X.C.; Zhou, M.F.; Kennedy, A.K.; Zi, J.W.; Spandler, C.; Yang, Y.H. Unraveling mineralization and multistage hydrothermal overprinting histories by integrated in situ U-Pb and Sm-Nd isotopes in a paleoproterozoic breccia-hosted IOCG deposit, SW China. *Econ. Geol.* **2021**, *116*, 1687–1710. [CrossRef]
50. Zhou, L.G.; Liu, J.P.; Li, J.; Sun, Z.B.; Xiang, L.; Zhou, Y.Y.; Tang, H.S.; Zhang, Y.B.; Zhu, X.Y.; He, H.L.; et al. Great Oxidation Event was caused by Neoarchean global cratonization: Opportunity and challenge from rock and sedimentary records in China. *Sci. Bull.* **2025**, *70*, 1736–1739. [CrossRef] [PubMed]
51. Zhou, M.F.; Yan, D.P.; Kennedy, A.K.; Li, Y.Q.; Ding, J. SHRIMP U-Pb zircon geochronological and geochemical evidence for Neoproterozoic arc-magmatism along the western margin of the Yangtze Block, South China. *Earth Planet. Sci. Lett.* **2002**, *196*, 51–67. [CrossRef]
52. Guo, Y.; Wang, S.W.; Sun, X.M.; Liao, Z.W.; Wang, Z.Z.; Zhou, B.G.; Yang, B. Zircon U-Pb Age of the Paleoproterozoic Diabase from the Yinachang Iron-copper Deposit, Yunan Province, and its Geological Implication. *Geotecton. Met.* **2014**, *38*, 208–215. (In Chinese with English abstract)
53. Zhou, M.F.; Zhao, X.F.; Chen, W.T.; Li, X.C.; Wang, W.; Yan, D.P.; Qiu, H.N. Proterozoic Fe–Cu metallogeny and supercontinental cycles of the Southwestern Yangtze block, Southern China and Northern Vietnam. *Earth Sci. Rev.* **2014**, *139*, 59–82. [CrossRef]
54. Chen, W.T.; Zhou, M.F.; Zhao, X.F. Late paleoproterozoic sedimentary and mafic rocks in the Hekou area, SW China: Implication for the reconstruction of the Yangtze block in Columbia. *Precambrian Res.* **2013**, *231*, 61–77. [CrossRef]
55. Chen, W.T.; Sun, W.H.; Wang, W.; Zhao, J.H.; Zhou, M.F. Grenvillian intra-plate mafic magmatism in the Southwestern Yangtze block, SW China. *Precambrian Res.* **2014**, *42*, 138–153. [CrossRef]
56. Shen, Y.T.; Yang, G.L.; Tan, H.B.; Wang, J.P.; Zhang, M.H.; Shen, C.Y. Review on Bouguer gravity anomaly and crustal density structure in Sichuan-Yunnan and its adjacent areas. *Rev. Geophys. Planet. Phys.* **2022**, *53*, 316–330. (In Chinese with English abstract).
57. Zhan, L.; Junlu, W.; Yaotian, Y.; Hui, C.; Miao, P.; Xianzhong, L.; Xiaofei, Z.; Bing, Y.; Longlong, L.; Sheng, X.; et al. Crustal electrical resistivity structure beneath the sediment-hosted stratiform Cu (SSC) deposits: A case study from Wuding area on the western margin of Yangtze Craton. *Ore Geol. Rev.* **2026**, *188*, 107080. [CrossRef]
58. Zhang, Y.H.; Liu, H.T.; Li, R.X. *Report on Stream Sediment Survey Results from the Mineral Prospectivity Survey of the Yimen Area, Yunnan Province*; Yunnan Provincial Bureau of Nonferrous Metals Geology: Yunnan, China, 2013; pp. 1–147. (In Chinese)
59. Li, Z.Q. Study on metallogenic geochemistry of iron and copper deposits in the Yinmin Formation of the Kungyang Group in the Middle Proterozoic Suberathem. *Miner. Resour. Geol.* **1996**, *10*, 100–107. (In Chinese with English abstract)
60. Selley, D.; Broughton, D.; Robert, S.; Hitzman, M.W.; Bull, S.; Large, R.; Peter, M.G.; Mawson, C.; Nicky, P. A new look at the geology of the Zambian copperbelt. *Econ. Geol.* **2005**, *100*, 965–1000.
61. Selley, D.; Scott, R.; Emsbo, P.; Koziy, L.; Hitzman, M.W.; Bull, S.W.; Duffett, M.; Sabagenzi, S.; Halpin, J.; Broughton, D.W. Structural configuration of the central African Copperbelt: Roles of evaporites in structural evolution, basin hydrology, and ore location. In *Metals, Minerals, and Society (Special Publication 21)*; Arribas, A.M., Mauk, J.L., Eds.; Society of Economic Geologists: Littleton, CO, USA, 2018; pp. 115–156.
62. Sośnicka, M.; Gigler, G.M.; Kinnaird, J.A.; Przybylowicz, W.J.; Chimvinga, J.; Master, S.; Plessen, B. Mineralizing fluids of the supergeneenriched Mashitu south Cu-Co deposit, Katanga copperbelt, DRC. *Ore Geol. Rev.* **2019**, *109*, 201–228. [CrossRef]
63. Turner, E.C.; Dabros, Q.; Broughton, D.W.; Kontak, D.J. Textural and geochemical evidence for two-stage mineralisation at the Kamoa-Kakula Cu deposits, Central African Copperbelt. *Miner. Depos.* **2023**, *58*, 825–832. [CrossRef]
64. Zhang, X.; Zhu, X.Y.; Jiang, H.; Lü, X.Q.; Wang, Y.F.; Liu, W.J.; Tian, L.P.; Zeng, R.Y.; Xiao, J. Metallogenic characteristics and prospecting direction of Dongchuan Copper Deposit, Yunnan Province. *Miner. Explor.* **2021**, *12*, 964–971. (In Chinese with English abstract).
65. Jackson, M.P.A.; Warin, O.N.; Woad, G.M.; Hudec, M.R. Neoproterozoic allochthonous salt tectonics during the Lufilian orogeny in the Katangan Copperbelt, central Africa. *Geol. Soc. Am. Bull.* **2003**, *115*, 314–330. [CrossRef]
66. Ruan, H.C.; Hua, R.M.; Cox, D.P. Copper deposition by fluid mixing in deformed strata adjacent to a salt diapir, Dongchuan area, Yunnan Province, China. *Econ. Geol.* **1991**, *86*, 1539–1545. [CrossRef]
67. Jiang, Q.L.; Huo, S.Y. *Report on the Verification of Resource Reserves in the Shizishan Copper Mine Verification Area, Yimen County, Yunnan Province*; Geological Exploration Institute, Yunnan Provincial Bureau of Nonferrous Metals Geology: Yunnan, China, 2010; pp. 1–95. (In Chinese)
68. Yin, X.Q.; Zhao, X.F.; Su, Z.K.; Lin, H.T.; Zhu, Z.M.; Song, W.L.; Martin, Y.H.L.; Zhao, K.D. Linking two types of breccias to sediment-hosted stratiform copper (SSC) and iron oxide-copper-gold (IOCG) deposits in the Kangdian metallogenic belt, SW China. *Miner. Depos.* **2025**, *60*, 1479–1502. [CrossRef]

69. Wang, L.; Ding, J.J.; Han, R.S.; Ren, T.; Li, C.; Zhu, E.Y.; Jiang, Z.H.; Huang, Y.H. Re-Os dating and S isotopic composition of chalcopyrite and bornite in the Shizishan copper deposit, Yimen, Yunnan Province. *Acta Geol. Sin.* **2021**, *95*, 837–851. (In Chinese with English abstract)
70. Li, Y.L. The Study of Geological-Geochemical Features and the Model of Ore-Controlling Structure in the Xikuangshan Type Copper-Ferro Deposit, Dongchuan, Yunnan Province. Master's Thesis, Kunming University of Science and Technology, Kunming, China, 2021. (In Chinese with English abstract)
71. Ye, L. The Geochemical Research of Xikuangshan Type Copper Ore Deposit, Dongchuan, Yunnan. Master's Thesis, Institute of Geochemistry, Chinese Academy of Sciences, Guiyang, China, 2004. (In Chinese with English abstract)
72. Zhao, X.F.; Zhou, M.F.; Li, J.W.; Liang, Q. Late Paleoproterozoic sedimentary rock-hosted stratiform copper deposits in South China: Their possible link to the supercontinent cycle. *Miner. Depos.* **2013**, *48*, 129–136. [CrossRef]
73. Wang, S.W.; Wang, Z.Z.; Guo, Y.; Sun, X.M.; Li, C.; Lu, S.L. Re-Os Isotopic Age of Massive Chalcopyrite in the Luoxue-Type Copper Deposit, Dongchuan, Yunnan. In Proceedings of the Abstracts of the 10th National Symposium on Metallogenic Theory and Prospecting Methods, Xi'an, China, 15–18 December 2023; p. 120. (In Chinese)
74. Qiu, H.N.; Wijbrans, J.R.; Li, X.H.; Zhu, B.Q.; Zhu, C.L.; Zeng, B.C. New 40Ar-39Ar evidence for ore-forming process during Jinning-Chengjiang period in Dongchuan type copper deposits, Yunnan. *Miner. Depos.* **2002**, *21*, 129–135. (In Chinese with English abstract).
75. Hahn, G.A.; Thorson, J.P. Geology of the Lisbon Valley sandstone hosted disseminated copper deposits. *Utah Geol. Assoc. Publ.* **2005**, *32*, 511–533.
76. Qin, D.X.; Tian, Y.L.; Yan, Y.F.; Lin, Y.B.; Liu, W. Geochemistry of the Shizishan Copper Deposits, Yimen, Yunnan. *Acta Geol. Sin.* **2000**, *74*, 72–84. (In Chinese with English abstract)
77. Li, Q. Research on Geology, Geochemistry and Concealed Deposit Prediction of Yimen Shizishan Copper Deposit. Master's Thesis, Kunming University of Science and Technology, Kunming, China, 2010. (In Chinese with English abstract)
78. Gao, H.; Pei, R.F.; Wang, A.J.; Cao, D.H.; Fan, S.J.; Mei, Y.X. Marine sand shale-hosted copper mineralization model and geological correlation: A case study of the Dongchuan copper mine in Yunnan and the Aynak copper mine in Afghanistan. *Geol. Bull. China* **2012**, *31*, 1332–1351. (In Chinese with English abstract)
79. Dai, H.Z.; Liu, J.J.; Zhu, W.B. Studies on tectonic setting, sedimentary environment and mineralization mechanism of the Yinmin copper deposit in Yunnan Province. *Earth Sci. Front.* **2018**, *25*, 108–124. (In Chinese with English abstract)
80. Taylor, C.D.; Causey, J.D.; Denning, P.D.; Hayes, T.S.; Horton, J.D.; Kirschbaum, M.J.; Parks, H.L.; Wilson, A.B.; Wintzer, N.E.; Zientek, M.L. *Descriptive Models, Grade-Tonnage Relationships, and Databases for the Assessment of Sediment Hosted Copper Deposits with Emphasis on Deposits in the Central African Copperbelt, Democratic Republic of the Congo and Zambia*; U.S. Geological Survey: Lawrence, KS, USA, 2013; pp. 1–154.
81. Brown, A.C. World-class sediment-hosted stratiform copper deposits: Characteristics, genetic concepts and metallotects. *Aust. J. Earth Sci.* **1997**, *44*, 317–328. [CrossRef]
82. Sillitoe, R.H.; Perello, J.; Garcia, A. Sulfide-bearing veinlets throughout the stratiform mineralization of the central African copperbelt: Temporal and genetic implications. *Econ. Geol.* **2010**, *105*, 1361–1368. [CrossRef]
83. Qiu, Z.J.; Fan, H.R.; Goldfarb, R.; Tomkins, A.G.; Yang, K.F.; Li, X.C.; Xie, L.W.; Liu, X. Cobalt concentration in a sulfidic sea and mobilization during orogenesis: Implications for targeting epigenetic sediment-hosted Cu-Co deposits. *Geochim. ET Cosmochim. Acta.* **2021**, *305*, 1–18. [CrossRef]
84. Perelló, J.; Wilson, A.; Wilton, J.; Creaser, R.A. Lufilian copper-gold mineralization in the Mkushi District, Zambia: Regional metallogenic implications. *Miner. Depos.* **2022**, *57*, 1089–1106. [CrossRef]
85. El Desouky, H.A.; Muchez, P.; Boyce, A.J.; Schneider, J.; Cailteux, J.L.H.; Dewaele, S.; Quadt, A.V. Genesis of sediment-hosted stratiform copper-cobalt mineralization at Luiswishi and Kamoto, Katanga Copperbelt (Democratic Republic of Congo). *Miner. Depos.* **2010**, *45*, 735–763. [CrossRef]
86. Cailteux, J.L.H.; Kampunzu, A.B.; Lerouge, C. The Neoproterozoic Mwashya-Kansuki sedimentary rock succession in the central African Copperbelt, its Cu-Co mineralisation, and regional correlations. *Gondwana Res.* **2007**, *11*, 414–431. [CrossRef]
87. Foltyn, K.; Węgrzynek, D.; Erlandsson, V.B.; Gugała, E.; Kozub-Budzyń, G.A.; Melcher, F.; Szczerbowska-Boruchowska, M.; Piestrzyński, A. Geochemical and mineralogical investigation of germanium-rich chalcopyrite veins from the Cu-Ag Kupferschiefer deposit, Poland. *Ore Geol. Rev.* **2025**, *181*, 106636. [CrossRef]
88. Chen, Y.D.; Liu, H.T. *Report on Geophysical and Geochemical Exploration Results from the Yimen County Tongchang–Xiaomaoshan Copper Deposit Key Inspection Area, Mineral Prospectivity Survey of the Yimen Area, Yunnan Province*; Yunnan Provincial Bureau of Nonferrous Metals Geology: Yunnan, China, 2012; pp. 1–89. (In Chinese)

Disclaimer/Publisher's Note: The statements, opinions and data contained in all publications are solely those of the individual author(s) and contributor(s) and not of MDPI and/or the editor(s). MDPI and/or the editor(s) disclaim responsibility for any injury to people or property resulting from any ideas, methods, instructions or products referred to in the content.